

# M Room Acoustics

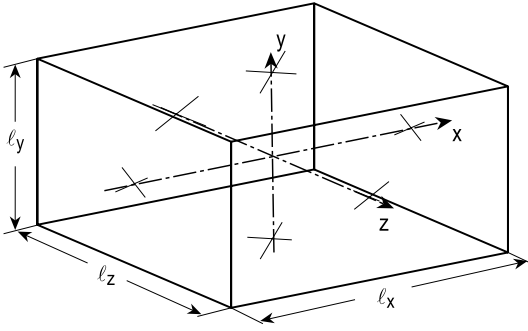
*with M. Vorländer*

Both deterministic and statistic methods of sound field evaluations in rooms will be described. Because of the complexity of room shapes and acoustic qualities of walls, evaluations in general will be approximative.

## M.1 Eigenfunctions in Parallelepipeds

---

Rooms with uniform, rectangular walls belong to the few examples in room acoustics in which a modal analysis can be performed with a reasonable amount of analytical and numerical work. As such they may serve as gauge objects for conceptions and methods.



The corner lengths are  $\ell_x, \ell_y, \ell_z$ , respectively. The wall surface admittances are  $G_x, G_y, G_z$ , if the walls on opposite sides are equal, otherwise  $G_{x1}, G_{x2}$ , etc.

The aim is to find elementary solutions (eigenfunctions or modes) with which sound fields for an arbitrary sound source in the room can be synthesised. They must obey the wave equation, symmetry conditions and boundary conditions.

Alternative writing:

$$x, y, z = x_1, x_2, x_3; \quad \ell_x, \ell_y, \ell_z = \ell_1, \ell_2, \ell_3; \quad G_x, G_y, G_z = G_1, G_2, G_3.$$

Wave equation:

$$\frac{\partial^2 p}{\partial x^2} + \frac{\partial^2 p}{\partial y^2} + \frac{\partial^2 p}{\partial z^2} + k_0^2 p = 0. \quad (1)$$

Fundamental solutions separate

$$p(x_1, x_2, x_3) = q_1(k_1 x_1) \cdot q_2(k_2 x_2) \cdot q_3(k_3 x_3) \quad (2)$$

with

$$q_i = \begin{cases} \cos(k_i x_i); & \text{symmetrical rel. } x_i = 0 \\ \sin(k_i x_i); & \text{anti-symmetrical rel. } x_i = 0 \end{cases} ; \quad i = 1, 2, 3. \quad (3)$$

They satisfy the wave equation if (*secular equation*):

$$k_0^2 \stackrel{!}{=} k_1^2 + k_2^2 + k_3^2. \quad (4)$$

If the room is symmetrical in the direction of  $x_i$  (i.e.  $G_{i1} = G_{i2} = G_i$ ) and the field is symmetrical (depending on the directivity and position of the source):  $q_i = \cos(k_i x_i)$ ; with room symmetry in the direction of  $x_i$  and anti-symmetrical field:  $q_i = \sin(k_i x_i)$ . Else:  $q_i = a_i \cos(k_i x_i) + b_i \sin(k_i x_i)$ .

The boundary conditions at the walls lead to the characteristic equations for  $k_i$ . Define

$$\begin{aligned} U_i &= (k_0 \ell_i / 2) \cdot Z_0 G_i && \text{for symmetrical walls,} \\ U_{i1} &= (k_0 \ell_i / 2) \cdot Z_0 G_{i1} ; \quad U_{i2} = (k_0 \ell_i / 2) \cdot Z_0 G_{i2} && \text{for anti-symmetrical walls.} \end{aligned}$$

General case (unsymmetrical room):

$$\text{With: } U_{si} = \frac{1}{2} (U_{i1} + U_{i2}); \quad U_{ai} = \frac{1}{2} (U_{i1} - U_{i2}),$$

the characteristic equation is written as:

$$\left[ (k_i \ell_i / 2) \cdot \tan(k_i \ell_i / 2) - j U_{si} \right] \cdot \left[ (k_i \ell_i / 2) \cdot \cot(k_i \ell_i / 2) + j U_{si} \right] \stackrel{!}{=} U_{ai}^2 \quad (5)$$

with the amplitude ratio of the anti-symmetrical to the symmetrical part of the mode:

$$\frac{b_i}{a_i} = -\cot(k_i \ell_i / 2) \frac{(k_i \ell_i / 2) \cdot \tan(k_i \ell_i / 2) - j U_{i2}}{(k_i \ell_i / 2) \cdot \tan(k_i \ell_i / 2) + j U_{i2}}. \quad (6)$$

*Special case:* symmetrical room ( $G_{i1} = G_{i2} = G_i$ ), symmetrical mode; characteristic equation:

$$(k_i \ell_i / 2) \cdot \tan(k_i \ell_i / 2) = j U_i. \quad (7)$$

*Special case:* symmetrical room ( $G_{i1} = G_{i2} = G_i$ ), anti-symmetrical mode; characteristic equation:

$$(k_i \ell_i / 2) \cdot \cot(k_i \ell_i / 2) = -j U_i. \quad (8)$$

*Special case:* both walls normal to  $x_i$  are hard ( $G_{i1} = G_{i2} = G_i = 0$ ), symmetrical mode:

$$k_i \ell_i / 2 = m_i \pi; \quad m_i = 0, 1, 2, \dots \quad (9)$$

*Special case:* both walls normal to  $x_i$  are hard ( $G_{i1} = G_{i2} = G_i = 0$ ), anti-symmetrical mode:

$$k_i \ell_i / 2 = (m_i + 1/2) \pi; \quad m_i = 0, 1, 2, \dots \quad (10)$$

In these equations  $G_i \neq 0$  may represent either a locally reacting or a bulk reacting wall. In the first case  $G_i$  is independent of  $k_i$ ; in the second case  $G_i = G_i(k_1, k_2, k_3)$ . In both

cases the modes are orthogonal (see ► *Sects. B.6 and B.7*) and as such are suited for field synthesis.

The three characteristic equations ( $i = 1, 2, 3$ ) and the secular Eq. M.1.(4) in general cannot be solved simultaneously for all frequencies. In the special case of only hard walls and symmetrical modes, one finds (with  $l = m_1, m = m_2, n = m_3$ ) eigenfrequencies  $f_{lmn}$ :

$$k_0^2 = (2\pi f_{lmn}/c_0)^2 = \sum_i k_i^2 = \sum_i (2\pi m_i/\ell_i)^2, \quad (11)$$

$$f_{lmn} = c_0 \sqrt{(l/\ell_1)^2 + (m/\ell_2)^2 + (n/\ell_3)^2}.$$

If the mode is anti-symmetrical in some direction  $x_i$ , substitute  $m_i \rightarrow m_i + 1/2$ .

In cases with  $G_i \neq 0$  the secular Eq. M.1.(4) with the solutions  $k_i$  of the characteristic equations must be solved numerically for eigenfrequencies. Under some restrictive conditions one can derive approximations. This will be shown for symmetrical, locally reacting walls and symmetrical modes, i.e. for Eq. M.1.(7). Write that equation as

$$z_i \cdot \tan z_i = j U_i = j k_0 \ell_i \cdot Z_0 G_i; \quad z_i = k_i \ell_i / 2. \quad (12)$$

With the continued-fraction expansion of  $\tan(z_i) = \tan(z_i - m_i\pi)$ ;  $m_i = 0, 1, 2, \dots$  writing

$$a_1 / (a_2 - a_3 / (a_4 - a_5 / (a_6 - \dots))) = \frac{a_1}{a_2 -} \frac{a_3}{a_4 -} \frac{a_5}{a_6 -} \dots,$$

one gets (see ► *Sect. J.7*),

$$z_i^2 = m_i \pi \cdot z_i + j k_0 \ell_i \cdot Z_0 G_i \cdot \left[ 1 - \frac{(z_i - m_i \pi)^2}{3 -} \frac{(z_i - m_i \pi)^2}{5 -} \dots \right] \quad (13a)$$

$$\xrightarrow{z_i \rightarrow m_i \pi} (m_i \pi)^2 + j k_0 \ell_i \cdot Z_0 G_i \xrightarrow{k_0 \ell_i \rightarrow 0 \text{ and/or } G_i \rightarrow 0} (m_i \pi)^2.$$

Thus:

$$k_i^2 = z_i^2 (2/\ell_i)^2 \approx 4 \frac{(m_i \pi)^2 + j k_0 \ell_i \cdot Z_0 G_i}{\ell_i^2}. \quad (13b)$$

This inserted into the secular equation gives an approximate equation for the eigenfrequencies (represented by  $k_0$ ):

$$k_0^2 - 4j k_0 (Z_0 G_1/\ell_1 + Z_0 G_2/\ell_2 + Z_0 G_3/\ell_3) - 4\pi^2 ((m_1/\ell_1)^2 + (m_2/\ell_2)^2 + (m_3/\ell_3)^2) \stackrel{!}{=} 0. \quad (14)$$

Similar procedures may be applied for other cases of symmetry. It should be noticed that the condition used  $z_i \rightarrow m_i \pi$  implies small admittance values  $|G_i|$ . But even this equation cannot be discussed further without knowledge of the functions  $G_i(k_0)$ .

In a formal manner one can write for the solutions (with  $k_{lmn} = 2\pi f_{lmn}/c_0$ ;  $f_{lmn}$  from Eq. M.1.(11)):

$$k_0 \rightarrow k_{lmn} = (\omega_{lmn} + j\delta_{lmn})/c_0, \quad (15)$$

where  $\delta_{lmn}$  represents a modal damping constant (which itself generally is complex).

Half-widths of modes (resonance curve):

$$(\Delta f)_{lmn} = \frac{\delta_{lmn}}{\pi}. \quad (16)$$

The transfer function between two points in a room is calculated by superposition of damped modes (resonance curves):

$$p(x_1, x_2, x_3, \omega) = \sum_{l,m,n} \frac{A_{lmn}(\omega)}{(\omega^2 - \omega_{lmn}^2 - 2j\delta_{lmn}\omega_{lmn})} \quad (17)$$

with  $\delta_{lmn} \ll \omega_{lmn}$  and  $A_{lmn}(\omega)$  depending on the source ( $x_{S1}, x_{S2}, x_{S3}$ ) and receiver positions ( $x_1, x_2, x_3$ ):

$$A_{lmn}(\omega) = \underline{p}_{lmn}(x_1, x_2, x_3) \underline{p}_{lmn}(x_{S1}, x_{S2}, x_{S3}) \int \int \int_V |\underline{p}_{lmn}(x_1, x_2, x_3)|^2 dx_1 dx_2 dx_3. \quad (18)$$

## M.2 Density of Eigenfrequencies in Rooms

Let  $N$  be the number of eigenfrequencies below the frequency  $f$ ; let  $n = dN/df$  be the number of eigenfrequencies in an interval of 1 Hz.

*Volume* with smallest corner length  $> \lambda_0/2$  ( $V$  = volume,  $S$  = room surface,  $L$  = sum of corner lengths,  $f$  = frequency):

$$N = \frac{4\pi V \cdot f^3}{3c_0^3} + \frac{\pi S \cdot f^2}{4c_0^2} + \frac{L \cdot f}{2c_0}, \quad (1)$$

$$n = \frac{4\pi V \cdot f^2}{c_0^3} + \frac{\pi S \cdot f}{2c_0^2} + \frac{L}{2c_0}.$$

*Flat volume* with smallest corner  $a < \lambda_0/2$ , other corners  $b, c > \lambda_0/2$ :

$$n = \frac{2\pi \cdot b \cdot c \cdot f}{c_0^2}. \quad (2)$$

*Tube* of length  $\ell$  with hard walls:

$$n = 2\ell/c_0. \quad (3)$$

The *mode overlap*  $m$  is defined as the ratio of the half-value bandwidth of a room resonance and the average frequency separation between neighbouring resonances around a frequency  $f$ . The mode overlap in the diffuse reverberant field is ( $T$  = reverberation time):

$$m = 0.69 \frac{V}{T} (f/1000)^2. \quad (4)$$

The mode overlap must exceed some lower limit value for the application of statistical methods in room acoustics. This defines a lower limit frequency  $f_s$  for such methods.

$$\text{Limit frequency for } m \geq 10: \quad f_s > 4000 \sqrt{T/V}. \quad (5)$$

Limit frequency for  $m \leq 10$ :  $f_s > 2000\sqrt{T/V}$ . (6)

The modulus of the room transfer function,  $|p(\omega)|$ , can be estimated by (see also Eq. M.1.(17)):

$$|p(\omega)| \approx \frac{|A_{lmn}|}{\sqrt{(\omega^2 - \omega_{lmn}^2)^2 + 4\omega^2\delta_{lmn}^2}}. \quad (7)$$

The probability density of the transfer function modulus  $z = |p(\omega)|$  (Rayleigh distribution) is:

$$P(z) dz = \frac{\pi}{2} e^{-\pi z^2/4} z dz, \quad (8)$$

and the probability density of transfer function phase  $\varphi = \arg(p(\omega))$  is:

$$P(\varphi) d\varphi = \frac{1}{2\pi} d\varphi. \quad (9)$$

### M.3 Geometrical Room Acoustics in Parallelepipeds

Assumptions:

- The room is a parallelepiped with corner lengths  $\ell_x, \ell_y, \ell_z$ .
- A small isotropic source is placed in the centre of the room.

Room volume:  $V = \ell_x \cdot \ell_y \cdot \ell_z$ . (1)

Walls:  $S_x = \ell_y \cdot \ell_z$ ;  $S_y = \ell_z \cdot \ell_x$ ;  $S_z = \ell_x \cdot \ell_y$ . (2)

Interior room surface:  $S = 2(S_x + S_y + S_z)$ . (3)

Number of mirror sources up to the order  $n = 1, 2, \dots$ :  $s_n = 4n^2 + 2$ . (4)

Positions of the mirror sources:  $\{\pm n\ell_x, \pm n\ell_y, \pm n\ell_z\}$ . (5)

Number of reflections including order  $n$ :  $\Sigma_n = \frac{2}{3}n(2n^2 + 3n + 4)$ . (6)

Estimation of temporal density of reflections [Cremer (1948)]:  $\frac{\Delta n(t)}{\Delta t} \approx \frac{4\pi c_0^3}{V} t^2$  (7)

and of the total number of reflections

between times 0 and  $t$ :  $n(t) \approx \frac{4\pi c_0^3}{3V} t^3$ . (8)

Mean free path length of sound:

energetic average:

$$\ell_{me}^2 = \lim_{n \rightarrow \infty} \frac{4n^2 + 2}{n^2} \bigg/ \sum_{i=12}^{4n^2+2} (1/\ell_{i,n}^2) \approx \frac{3}{4} \left[ \frac{1}{\ell_x^2 + \ell_y^2} + \frac{1}{\ell_y^2 + \ell_z^2} + \frac{1}{\ell_z^2 + \ell_x^2} \right]^{-1}, \quad (9)$$

geometrical average:

$$\ell_{\text{mg}} = \lim_{n \rightarrow \infty} \frac{1}{n} \sum_{i=1}^{4n^2+2} \frac{\ell_{i,n}}{4n^2+2} \approx \frac{1}{6} \left[ \sqrt{\ell_x^2 + \ell_y^2} + \sqrt{\ell_y^2 + \ell_z^2} + \sqrt{\ell_z^2 + \ell_x^2} \right]. \quad (10)$$

Value, often used in room acoustics [Kosten (1960)]:  $\ell_{\text{ma}} \approx 4V/S.$  (11)

(Effective) intensity of the direct sound field:

( $\Pi_q$  = effective power of source,  $d$  = distance source to receiver)

$$I_D = \frac{\Pi_q}{4\pi d}. \quad (12)$$

Intensity of reverberant field:

$$I_R = \sum_{n=1}^{\infty} I_{Rn} = \Pi_q \sum_{n=1}^{\infty} \frac{(1 - \bar{\alpha})^n (4n^2 + 2)}{4\pi n^2 \ell_{\text{me}}^2} \xrightarrow{\bar{\alpha} < 0.1} \Pi_q \frac{1 - \bar{\alpha}}{\pi \bar{\alpha} \ell_{\text{me}}^2} \quad (13)$$

with

$$S \cdot \bar{\alpha} = \sum \alpha_i S_i. \quad (14)$$

Intensity of reverberant field, including absorption of air:

$$I_R = \frac{\Pi_q}{\pi \ell_{\text{me}}^2} \frac{(1 - \bar{\alpha}) \cdot e^{-\beta \ell_{\text{me}}}}{1 - (1 - \bar{\alpha}) \cdot e^{-\beta \ell_{\text{me}}}} \approx \frac{\Pi_q}{\pi \ell_{\text{me}}^2} \frac{1 - \bar{\alpha} - \beta \ell_{\text{me}}}{\bar{\alpha} + \beta \ell_{\text{me}}}. \quad (15)$$

Approximation for  $\bar{\alpha} > 0.1$ :

$$I_R \approx \Pi_q \frac{1 - \bar{\alpha}}{\pi \ell_{\text{me}}^2} \left[ \frac{2}{\bar{\alpha}} + \frac{\pi^2}{6} \right] \approx \Pi_q \frac{(1 - \bar{\alpha})(6 + 5\bar{\alpha})}{3\pi \bar{\alpha} \ell_{\text{me}}^2}. \quad (16)$$

Level steps in reverberation plot:

$$\Delta L_1 = 10 \cdot \lg \left[ 1 + \frac{3\bar{\alpha} \ell_{\text{me}}^2}{2d^2(1 - \bar{\alpha})(6 + 5\bar{\alpha})} \right] [\text{dB}], \quad (17)$$

if an order of reflection is missing (independent of  $n!$ ):

$$\Delta L_2 = -10 \cdot \lg(1 - \bar{\alpha}) [\text{dB}]. \quad (18)$$

Decay rate (slope of level decay):  $m = -\Delta L \frac{c_0}{\ell_{\text{me}}}. \quad (19)$

Reverberation time:  $T = -60/m. \quad (20)$

## M.4 Statistical Room Acoustics

The diffuse sound field is a scientific artefact; it is a model for sound fields in large rooms.

$Z_0 = p_0 c_0$	= free field wave impedance;
$r$	= distance source to field point;
$Q$	= source directivity;
$w$	= energy density;
$A$	= total absorption area;
$V$	= room volume;
$S$	= room interior surface area;
$a, b, c$	= corner lengths of a cubic room;
$\bar{\alpha}$	= average absorption coefficient;
$S_i$	= absorber surface areas;
$\alpha_i$	= absorption coefficient of $S_i$ ;
$\beta$	= propagation attenuation of power;
$d$	= distance of limit between direct and reverberant field

A sound field is said to be diffuse if *on average over some time interval* the effective sound intensity (as a vector) in any field point is omnidirectional with constant magnitude for all directions. An immediate consequence is a zero effective power through a (small) reference volume around a field point. Without the permission of a finite time averaging the necessary consequence would be a zero sound field.

Energy balance in steady state conditions [Kuttruff (2000)]:

$$V \frac{dw}{dt} = \Pi_q - V \cdot \bar{n} \cdot \bar{\alpha} \cdot w \quad (1)$$

with  $\bar{n}$  denoting the average reflection rate, i.e. the expected number of reflections per time unit. It is calculated from the mean free path (Eq. M.3.(11)) by:

$$\bar{n} = \frac{c_0}{\ell_{ma}}. \quad (2)$$

The energy components in parallelepiped rooms can be related to reflections which depend on room shape, the reflection rate and wall absorption. The expectation value of the magnitude of the intensity of a reflection of order  $i$  is:

$$\langle I(t) \rangle = \frac{\Pi_q}{4\pi(c_0 t)^2} (1 - \bar{\alpha})^i, \quad (3)$$

where  $\bar{\alpha}$  denotes the average absorption coefficient. With the mean reflection rate  $\bar{n}$  it follows:

$$\langle I(t) \rangle = \frac{\Pi_q}{4\pi(c_0 t)^2} (1 - \bar{\alpha})^{\bar{n}t}. \quad (4)$$

In a diffuse field the intensity vectors are independent of the direction. Therefore the total sound field is obtained by superposition of incoherent contributions of intensity

moduli. With the number of reflections per time interval  $dt$  as given in [Sect. M.3](#) above (Eq. M.3.(7)), the total time-differential intensity is:

$$\left\langle \frac{dI(t)}{dt} \right\rangle = \frac{c_0 \cdot \Pi_q}{V} (1 - \bar{\alpha})^{\bar{n}t}. \quad (5)$$

The expectation value of the total time-differential energy density,  $dw(t)$ , is accordingly (differential energy density impulse response or: energy time curve):

$$\left\langle \frac{dw(t)}{dt} \right\rangle = \frac{\Pi_q}{V} (1 - \bar{\alpha})^{\bar{n}t}. \quad (6)$$

The energy density is thus:

$$\langle w \rangle = \int_{t_0}^{\infty} \frac{\Pi_q}{V} (1 - \bar{\alpha})^{\bar{n}t} dt \quad (7)$$

with  $t_0 = 0$ , and  $\bar{n}$  according to Eq. M.3.(11) yields:

$$\langle w \rangle = \frac{4\Pi_q}{c_0 S \bar{\alpha}}, \quad (8)$$

which can also be expressed in terms of the mean sound pressure  $\left( \overline{|p|^2} = Z_0 c_0 \langle w \rangle \right)$

$$\overline{|p|^2} = Z_0 c_0 \langle w \rangle = \frac{4Z_0 \Pi_q}{S \bar{\alpha}} = \frac{4Z_0 \Pi_q}{A}. \quad (9)$$

With  $t_0 = 1/\bar{n}$  (see Eq. M.4.(2)) this yields:

$$\overline{|p|^2} = \frac{4Z_0 \Pi_q}{S \bar{\alpha}} (1 - \bar{\alpha}) = \frac{4Z_0 \Pi_q}{A} (1 - \bar{\alpha}). \quad (10)$$

More generally, including air attenuation as well as wall absorption:

$$\langle dw(t) \rangle = \frac{\Pi_q \cdot dt}{V} (1 - \bar{\alpha})^{\bar{n}t} e^{-\beta_0 c_0 t}, \quad (11)$$

and again, with  $t_0 = 1/\bar{n}$ :

$$\overline{|p|^2} = \frac{4Z_0 \Pi_q}{S \bar{\alpha}} e^{-A/S} = \frac{4Z_0 \Pi_q}{A} e^{-A/S}. \quad (12)$$

The relation between the sound pressure  $p(r)$  at a field point with distance  $r$  to the source of a diffuse sound field and the effective power  $\Pi_q$  of a (small) source is:

$$\overline{|p(r)|^2} = Z_0 c_0 \Pi_q \left[ \frac{Q}{4\pi r^2} + \frac{4}{A} e^{-A/S} \right] \quad (13)$$

with  $Q$  being the directivity of the source.

$$A = S \bar{\alpha} + 4\beta V \quad \text{is the equivalent absorption area} \quad (14)$$



$$S\bar{\alpha} = \sum_i S_i \alpha_i . \quad (15)$$

Expectation of level decay:

$$L(t) = L_0 + 4.34 \bar{n} t \cdot \ln(1 - \bar{\alpha}) \text{ [dB]} . \quad (16)$$

Decay rate (slope of the level decay):

$$m = 4.34 \bar{n} \cdot \ln(1 - \bar{\alpha}) . \quad (17)$$

Reverberation times (for level decay over 60 dB):

$$T = -\frac{60}{4.34 \bar{n} \ln(1 - \bar{\alpha})} , \quad (18)$$

according to *Eyring*

$$T_{\text{Ey}} = -\frac{24 \ln(10)}{c_0} \frac{V}{S \ln(1 - \bar{\alpha})} , \quad (19)$$

$$T_{\text{Ey}} = \frac{60V}{-1.086 c_0 S \cdot \ln(1 - \bar{\alpha})} = -0.161 \frac{V}{S \cdot \ln(1 - \bar{\alpha})} ; \quad (20)$$

according to *Sabine*:

$$T_{\text{Sab}} = \frac{60V}{1.086 c_0 \sum \alpha_i S_i} = 0.161 \frac{V}{S \cdot \bar{\alpha}_{\text{Sab}} + 4\beta V} ; \quad (21)$$

according to *Millington-Sette*:

$$T_{\text{MS}} = \frac{60V}{-1.086 c_0 \sum S_i \cdot \ln(1 - \alpha_i)} = -0.161 \frac{V}{\sum S_i \cdot \ln(1 - \alpha_i)} ; \quad (22)$$

according to *Pujolle* (for rectangular rooms):

$$T_{\text{Pu}} = -\frac{6\ell_{\text{mg}}}{c_0 \log(1 - \bar{\alpha})} \approx -\frac{\sqrt{\ell_x^2 + \ell_y^2} + \sqrt{\ell_y^2 + \ell_z^2} + \sqrt{\ell_z^2 + \ell_x^2}}{c_0 \log(1 - \bar{\alpha})} ; \quad (23)$$

according to *Pujolle* (for rectangular rooms) including absorption of air:

$$T_{\text{Pu}} = \frac{13.8\ell_{\text{mg}}}{c_0 [\beta\ell_{\text{mg}} - \log(1 - \bar{\alpha})]} = \frac{6\ell_{\text{mg}}}{c_0 [0.43\beta\ell_{\text{mg}} - \log(1 - \bar{\alpha})]} . \quad (24)$$

The distance,  $d$ , of the limit between the direct and the reverberant field is determined by the equilibrium of direct and reverberant sound (Eq. M.4.(13)):

$$d = \sqrt{\frac{QA}{16\pi}} e^{A/S} = 0.1 \sqrt{\frac{QV}{\pi T}} e^{A/S} \quad (25)$$

or, in approximation of low absorption ( $A \ll S$ ):

$$d = \sqrt{\frac{QA}{16\pi}} = 0.1 \sqrt{\frac{QV}{\pi T}} . \quad (26)$$

## M.5 The Mirror Source Model

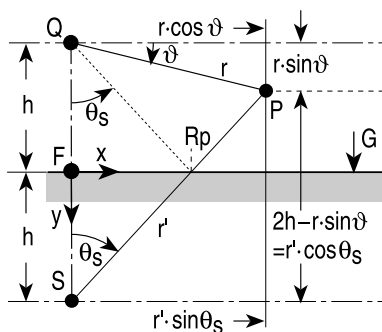
► *See also:* Mechel (2002)

The task is the evaluation of the sound pressure at a receiver point P inside a room for a simple source placed at Q. Analytically the sound field must satisfy the source condition (e.g. agreement of volume flow of the field at source position with volume flow of the source) and the boundary conditions (matching of field admittance with wall admittance) at all room walls. Analytical solutions, however, are possible only for very simple room geometries (see ▶ Sect. M.3). The classical tool for sound field evaluations in room acoustics is the *mirror source model*. It will be displayed here in some detail, going farther than the usual textbook example of parallelepipedic rooms. The mirror source model is often unjustly said to be inapplicable in practical tasks due to the supposedly enormous number of mirror sources which it is said to need. One can find in the literature the number  $n_w(n_w - 1)^{(o-1)}$  of mirror sources “needed” for the reflection order  $o$  in a room with  $n_w$  walls (e.g. 27 000 mirror sources for the low numbers of  $n_w = 6$  walls up to order  $o = 4$ ). It will be shown that the number of sources actually needed is much smaller. The mirror sources here will be described as a sequence of algorithms and programming rules for their evaluation, most of them being very elementary.

The word “mirror source” will be abbreviated as MS because of its frequent occurrence. The word “source” and the symbol  $q$  may denote both the original source  $Q$  and a mirror source (mostly symbolised by  $S$ ). Sometimes we speak of a “mother source” which creates at a wall (or “reflecting wall” if necessary) a “daughter source”.

### M.5.1 Foundation of Mirror Source Approximation

The MS method is exact only for a single, infinite, plane wall with ideal reflection (either hard or soft). Then the superposition of the fields of source Q and MS S satisfy the boundary condition at the wall. (See [▶ Sects. D.15 through D.20](#)).



The analysis of that elementary task returns the result for the reflected field  $p_r$ :

$$p_r(r', \theta_s) \xrightarrow[k_0 r' \gg 1]{} R(\theta_s) \cdot \begin{cases} H_0^{(2)}(k_0 r'); & \text{line source} \\ h_0^{(2)}(k_0 r'); & \text{point source} \end{cases} \quad (1)$$

with  $H_0^{(2)}(z)$  zero-order cylindrical Hankel function of second kind;

$h_0^{(2)}(z)$  zero-order spherical Hankel function of second kind.

$R(\theta_s)$  is the reflection factor of a plane wave incident on the wall under the angle which the connection of the mirror point S with the field point P includes with the normal to the wall. The forms (Eq. M.5.(1)) do not satisfy the wave equation if  $R(\theta_s) \neq \text{const}(\theta_s)$  because an azimuthal factor strictly cannot be associated with a Hankel function of zero order. This should also be kept in mind if the original source has a directivity factor  $D(\vartheta)$  (in 2D) or  $D(\vartheta, \varphi)$  (in 3D).

This is the *MS approximation*. One should keep in mind the following:

- The MS solution is only approximate if  $R(\theta_s) \neq \text{const}(\theta_s)$ , i.e. for  $G \neq 0$  or  $|G| \neq \infty$ .
- Then it violates the wave equation.
- It determines precisely the meaning of  $R(\theta_s)$ !
- With that definition (and only with that definition) it satisfies the wall boundary condition.
- It supposes  $k_0 r' \gg 1$ , i.e. large distances  $\text{dist}(S, P)$ , or more precisely: a great sum of the heights of Q and P over the wall.
- It supposes that P is not under an angle  $\theta_s$  with a strong angular variation of  $R(\theta_s)$ .
- For grazing incidence, i.e. Q and P on the wall, the influence of higher terms  $R^{(n)}(\theta_s)$  in Eqs. (D14.10) or (D20.11) is important!
- The derivation further supposes that the wall does not guide a surface wave [but this is only rarely the case in a restricted frequency range below a high-quality resonance; but even then Eq. M.5.(1) is an approximation to the field in points not too close to the wall].

The mentioned facts have important consequences:

- On the one hand, it makes no sense to try to compute with a higher precision than the precision of the fundamental process of the MS method.
- On the other hand, the approximate character of this process does not give a justification to fantastic modifications of the MS method.

## M.5.2 General Criteria for Mirror Sources

Mirror sources are created at a wall by a source which is on the *interior side* of the wall by the steps:

- Mirror-reflect the source position to behind the wall.
- Multiply its source factor by  $R(\theta_s)$ .
- If the source has a directivity factor  $D(\vartheta)$ , reflect that directivity, i.e. rotate it.

The continued multiplication, for increasing order  $o$  of reflection, creates a product of reflection factors  $R(\theta_s)$ , which will be called the “*source factor*” and symbolised by  $\Pi R$ .

The form of the MS and the co-ordinates used should, if possible, be such that these steps can be performed easily in the computations.

The right of a MS to exist is the satisfaction, together with its mother source, of the boundary condition at the wall at which it was created by its mother source – nothing else!

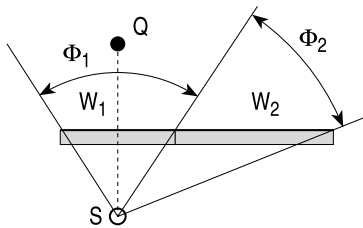
The first criterion for the generation of a daughter MS at a wall is that the mother source irradiates the interior surface of that wall. As a consequence, if a source is outside a wall, it does not create a daughter source at that wall. We call this rule the “*inside criterion*”. The chain of MS production is terminated if this criterion is violated; otherwise the daughter source would be “*illegal*” (see below for other criteria of interruption of MS

generation). In particular, a MS will never be mirror-reflected back to the position of its mother source.

### M.5.3 Field Angle of a Mirror Source

The *field angle* of a MS gives a further important criterion for the interrupt of MS production. The field angle is explained for the case of reflection of a source Q at a plane wall which is subdivided into two sections with different reflection factors  $R_i$  in them.

Although the source Q has only one position S for a MS, there are indeed positioned two MSs with different angular ranges  $\Phi_1, \Phi_2$  of their fields because there are two different source factors  $R_1, R_2$  in both ranges.



The field is unsteady at the common flank of the field angles. This is a consequence of the character of the MS method as an approximate solution which must be tolerated. In 3D the field angle  $\Phi$  is given by a polygonal pyramid subtended by a wall W (or wall section) and with the source S in the apex.

The “*field angle criterion*” states two things:

- A MS creates in P a field contribution only if P is in its field angle (more precisely: ...and on the interior side of the creating wall); otherwise we say “*the MS is ineffective*”.
- A MS generates a daughter MS at a wall W only if that wall is inside the range of its field angle (again, on the interior side of the creating wall); otherwise no boundary condition must be satisfied at W for MS, and therefore the daughter MS would be “*illegal*”.

The additions “on the interior side” in parentheses will be important for convex corners (see below). One can describe the effect of the field angle with the word “*visibility*”. A source q sees an object only if that object is inside its field angle. If q does not see P, then q is ineffective; if q does not see a wall W, then q does not produce a daughter source with W.

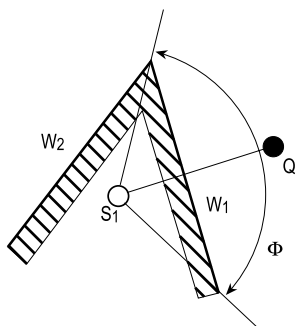
The chain of MS generation for increasing order of reflection is continued for an ineffective MS (because a daughter MS may become effective), but the chain is terminated at an illegal MS.

Some problems are caused by walls W which are only partially inside  $\Phi$ . In a strict procedure one would have to subdivide the wall at the intersection with the flank of  $\Phi$ , but such a “dynamical” definition of walls would produce much computational work. It is sufficient, within the framework of precision of room acoustical computations, to check

whether the wall section inside  $\Phi$  exceeds some size limit (e.g.  $\lambda_0$ ); if not, that wall is neglected for that MS. It is a good compromise between precision and computation load to check whether the centre  $C$  of  $W$  is inside  $\Phi$ . This check is done by a repeated test whether  $C$  is inside the walls of the polygonal pyramid with the MS at its apex and subtended by  $W$ . The repetition can be interrupted if  $C$  is outside one of the pyramid walls.

In general, MSs with increasing order are displaced farther and farther away from the interior of the considered room. Thus their field angles become smaller and smaller; so fewer walls have to be considered for the production of further MSs with increasing order of reflection.

The mentioned additional condition that either  $P$  or another wall must be in the field angle on the interior side of the generating wall is important, as can be seen from the next figure.

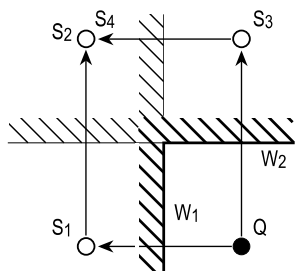


Here the source  $Q$  creates at  $W_1$  a MS,  $S_1$ , which in the depicted case is outside both walls  $W_1$ ,  $W_2$ . The inside criterion would interrupt a further production of MSs anyway. If, however,  $Q$  is displaced farther away from the wall  $W_1$ , then  $S_1$  may fall on the interior side of  $W_2$ . Nevertheless  $S_1$  will not produce a MS at  $W_2$  because  $W_2$  would be in  $\Phi$  but not on the interior side of the generating wall  $W_1$ .

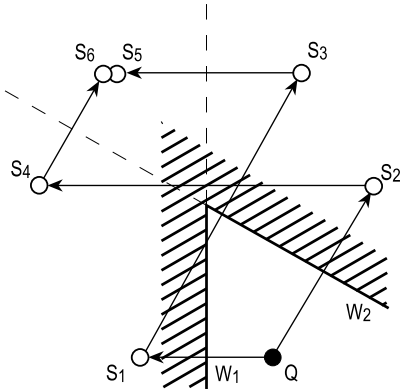
The additional condition ( $W_2$  inside  $W_1$ ) is relevant only for convex corners.

### M.5.4 Multiple Covering of MS Positions

In the first sketch of ► Sect. M.5.3 two MSs occupy the same position; both are legal; they are different from each other. If two walls form a space wedge, and if the wedge angle  $\Theta$  of two walls is a rational multiple of  $\pi$ , the MS beginning with some higher order will fall upon positions of MSs of lower orders, so they again occupy same positions.



The outer sides of the (possibly extended) walls are hatched. The chain of the MS production ends with  $S_2, S_4$  because both MSs are outside both walls. The source factors of both MS  $S_2$  and  $S_4$  are equal. Such coincident MSs with the same source factors are illegal because they violate the source condition of the boundary value problem

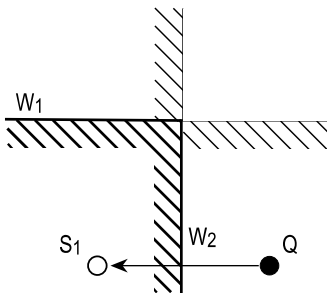


In this example the MS production ends with  $S_5, S_6$  because both MSs are outside both walls.

Depending on the wedge angle  $\Theta$  and on the position of  $Q$ , different numbers of MSs can be constructed (higher for small  $\Theta$ , infinitely high for parallel walls, i.e. for  $\Theta = 0$ ).

### M.5.5 Convex Corners

Convex corners, i.e. with wedge angles  $\Theta > \pi$ , cannot be treated with the “traditional” MS method. Only one MS can be constructed at this convex rectangular corner. That is evidently not enough to represent the sound field at such a corner. Consequently, the traditional MS method fails at convex corners!



### M.5.6 Interrupt Criteria in the MS Method

The MS method is often blamed for the apparent exorbitantly high numbers of MSs involved. In such statements inherent interruption criteria of the MS method are ignored.

Conditions for the interrupt of the chain of MS production are as follows:

- 1) The source  $q$  is outside the mirror wall  $W$ :  
there exists no boundary condition for  $q$  at  $W$ ;  
the MS chain must be interrupted.
- 2) A wall  $W$  is outside the field angle  $\Phi$  of  $q$ :  
 $q$  does not produce a daughter MS at  $W$ .  
For walls with a common corner this is equivalent to 1).
- 3) A MS would fall within the interior room space:  
then there would be, except for  $Q$ , a new pole position of the field;  
this violates the condition of regularity of the field outside  $Q$ .  
This case is encountered in the case of convex corners only.
- 4) If the new MS falls on  $Q$ :  
from then on the MS positions would be repeated;  
this violates the source condition which demands that the volume flow through a small enclosure around  $Q$  must be the same as that of the original source.
- 5) The product  $\Pi|R|$ , which is the source factor of  $q$ , would become  $< \text{limit}$ , which is a preset limit. This would make the field contribution negligible, also for all daughter sources of  $q$ .
- 6) If the sound field is the target quantity, the distance  $\text{dist}(q, P)$  of a source  $q$  from  $P$  may be restricted to being  $< d_{\text{max}}$ . For point sources the amplitude ratio of  $q$  at  $P$ , relative to the amplitude of  $Q$  at  $P$ , is  $\text{dist}(Q, P)/\text{dist}(q, P)$ . This ratio generally becomes even smaller for daughter sources of  $q$ .
- 7) A limitation  $\Pi|R| \cdot \text{dist}(Q, P)/\text{dist}(q, P) < \text{limit} \cdot d_{\text{max}}$  would be more significant.
- 8) With some arbitrariness one sets an upper limit of the orders  $o = 1, 2, \dots, o_{\text{max}}$  of the MS.

In interrupt checks using  $\Pi|R|$  it may be sufficient to use approximate values for the reflection factors  $R$  (or their magnitudes  $|R|$ ), for example the reflection factor for normal sound incidence, or the reflection coefficient  $|R|^2$  from the absorption coefficient for diffuse sound incidence. Then the construction of the MS becomes independent of the position of  $P$ . The reflection factors are the only quantities which introduce the frequency into the construction of the MS. If one takes for the interruption check a lower limit or an average value of  $|R|$  over the frequency interval considered, the construction of the MS is also independent of the frequency. One should apply tests with the true  $|\Pi R|$  while evaluating the field contributions of the sources, when the IIR are available. In the phase of field evaluation these tests must be applied on a smaller number of MSs than in the phase of MS construction.

### M.5.7 Computational Parts of the MS Method

The traditional MS method consists of three computational parts:

- Find the positions of the MS (considering the inside and field angle criteria).
- Determine the source factors of the MS, i.e. of the reflection factors  $R(\theta_s)$  (depending on the acoustical quality of the mirror wall and of the relative positions of the MS and P).
- Evaluate the contributions of the MS to the field at P.

Most programming is needed to find the MS positions, although the single steps are elementary geometrical tasks. Less intensive in programming is the evaluation of the reflection factors of absorbent walls. This task may be delegated to subroutines for the wall surface admittance  $G$ . Most simple is the evaluation of the field contributions; only a number of Hankel functions of zero order must be evaluated; this subtask is fast computing for spherical Hankel functions (which are given by  $\cos(x)$ ,  $\sin(x)$ ) and is fast computing also for cylindrical Hankel functions when using the known polynomial approximations for Bessel and Neumann functions of zero order.

The computational MS method proceeds with the order  $o$  of mirror reflections.

- At the order  $o = 1$  the MSs  $S(1)$  are determined in turn for all walls (consider the inside criterion for convex corners!).
- At the order  $o = 2$  all  $S(1)$  are potential mother sources for the generation of the MSs of the second order  $S(2)$  at all walls (except for the wall at which  $S(1)$  was produced) unless the inside and field angle criteria exclude  $S(2)$ .
- Continue until a final interrupt criterion is met.

### M.5.8 Inside Checks

Checks for interruption and efficiency form the main part of the computational work in the computational MS method. They are fundamental tasks of computational geometry. But because they are repeated very often, they should compute fast. We break down all geometrical tests into “inside checks”. An inside check examines whether a point  $q$  is on the interior side of a wall plane, in the wall plane, or on the exterior side of the wall plane (the sides are defined by the rotational sense of the edges  $E_k$  of a wall  $W = \{E_1, E_2, E_3, \dots\}$ ). One could do the inside check with the help of direction cosines of the connecting lines between  $q$  and the  $E_k$ . The evaluation of angles, however, is slow. An inside check in 3D uses the vector triple product (scalar product of a vector and a vector product) if the wall  $W$  is given by three of its edges. If the parameters  $a, b, c, d$  of the reduced normal form of the wall equation

$$a \cdot x + b \cdot y + c \cdot z + d = 0 \quad (2)$$

are known, the inside check needs three multiplications and three additions (see appendix) with  $q = \{x, y, z\}$ :

$$a \cdot x + b \cdot y + c \cdot z + d \begin{cases} > 0; & q \text{ inside the } W \text{ plane} \\ = 0; & q \text{ on the } W \text{ plane} \\ < 0; & q \text{ outside the } W \text{ plane} \end{cases}, \quad (3)$$

if the edges of  $W$  and  $q$  form a right-handed system; otherwise the signs change.



Another, often used, test examines if a point  $P$  is inside the polygonal pyramid which has the point  $q$  as apex and is subtended by a wall  $W$ . This test is done by a repetition of inside checks for  $P$  and the triangles forming the sides of the pyramid. The loop over the triangles can be aborted with a negative answer for the test if one of the inside checks fails (distinguish whether  $W$  and  $q$  are a right-handed or left-handed system).

The shading of a point  $P$  or a wall  $W$  by a convex corner and the visibility of  $P$  or  $W$  from a point  $q$  through an aperture (formed by convex corners with a free interspace between them) are also tested with inside checks.

### M.5.9 What Is Needed in the Traditional MS Method?

One needs as input the following:

- the list of walls  $\{W_1, W_2, W_3, \dots\}$ , which themselves are lists of edges  $W_w = \{E_{w1}, E_{w2}, E_{w3}, \dots\}$ ,  $E_i = \{x_i, y_i, z_i\}$ ;
- the source point  $Q = \{x_Q, y_Q, z_Q\}$ ;
- the field point  $P = \{x, y, z\}$ ;
- the list of wall admittances  $G = \{G_1, G_2, G_3, \dots\}$ ;
- the limits  $o_{\max}$ , limit,  $d_{\max}$  for the order  $o$ , the source factors  $|\Pi R|$ , and  $\text{dist}(q, P)$ , respectively.

It is supposed that the  $\text{dist}(Q, P)$ , the wall centres  $C_w$ , and the parameters  $a, b, c, d$  of the reduced normal forms of the wall equations  $a \cdot x + b \cdot y + c \cdot z + d = 0$  are evaluated (see appendix). One needs, for the evaluation of the reflection factors and of the contributions in  $P$  the following:

- 1) position  $q$  of a source (either  $Q$  or a MS);
- 2) counting index  $w$  of the wall  $W$  at which  $q$  was generated;
- 3) distance  $\text{dist}(q, P)$ ;
- 4) amplitude factor  $\Pi R(\theta_s)$ ;
- 5) a flag which signals with  $\text{flag} = 0$  that  $q$  is an effective source (i.e. with a field contribution in  $P$ ) and with  $\text{flag} = 1$  that  $q$  is ineffective (no field contribution).

These data are collected in "source lists"  $\{q, w, \text{dist}(q, P), \Pi R(\theta_s), \text{flag}\}$ , and the source lists for a given order  $o = 0, 1, 2, \dots, o_{\max}$  are collected in tables

$\text{tab}(o) = \{\dots, \{q, w, \text{dist}(q, P), \Pi R(\theta_s), \text{flag}\}, \dots\}$ .

Let the counting index of a source list within  $\text{tab}(o)$  be  $s$ . The source table for the order  $o = 0$ , i.e. for the original source  $q = Q$ , has the form  $\text{tab}(0) = \{\{Q, 0, \text{dist}(Q, P), 1, 0\}\}$  for rooms with concave corners (see below for rooms with convex corners).

One can delegate the task of mirror reflection of a mother source  $q_m$ , represented by its source list  $\{q_m, w_m, \text{dist}(q_m, P), \Pi_m R(\theta_s), \text{flag}_m\}$ , at a wall  $W_w$ , given by its index  $w$ , including all tests of interrupt and effectivity, to a subroutine, which should be carefully checked and economised with respect to computing time. That subroutine returns

- the source list  $\{q, w, \text{dist}(q, P), \Pi R(\theta_s), \text{flag}\}$  of the daughter source if no interrupt criterion is met;
- the value 0 if an interrupt criterion is met.

Such a subroutine for 3D rooms with concave corners is a program of about 25 program lines in the Mathematica<sup>®</sup> language (the geometrical subtasks inside the subroutine are delegated to subroutines).

The traditional MS method works in three nested loops:

- 1) The outer loop over the order  $o = 1, 2, \dots, o_{\max}$ :  
it produces the source table  $\text{tab}(o)$ .
- 2) The middle loop over the counting index  $s = 1, 2, \dots$  of the sources in  $\text{tab}(o - 1)$ .
- 3) The innermost loop over the counting index  $w = 1, 2, \dots$  of walls;  
it calls the above-mentioned subroutine;  
if that subroutine does not return 0, the new source list is appended to  $\text{tab}(o)$ .

This traditional MS method is attractive for its computational simplicity. A frame program for the evaluation of the  $\text{tab}(o)$  in Mathematica<sup>®</sup> typically is a program of about 12 lines, if the frame program calls a subroutine for the MS evaluation with all checks inside the subroutine. It may be of some advantage to perform the checks of legitimacy of a new MS (mother source inside the mirror wall; mirror wall in the field cone of the mother source) in the frame program (this is true especially when the MS method is applied to rooms with convex corners).

The returned tables  $\text{tab}(o)$  also contain ineffective sources ( $\text{flag} = 1$ ). One can select the effective sources with  $\text{flag} = 0$  and collect them in tables  $\text{tabeff}(o)$ . So one has available all data which are needed to evaluate and sum up the field contributions in  $P$  of the effective sources.

### M.5.10 The Object

The geometrical object is a room formed by plane walls  $W_w$ . What is inside and outside of the room is clearly defined. The (original) source  $Q$  and the field point  $P$  are always inside. A right-handed Cartesian system of co-ordinates  $x, y, z$  is laid over the room.

The walls  $W_w$  are plane. They are described by lists of edges,  $W_w = \{E_{w1}, E_{w2}, E_{w3}, \dots\}$ , which are ordered such that the sense of rotation in that order and the direction pointing to the inside of the room make a right-handed system. Because the first three edges are used for the determination of the unit normal vector of the wall, these edges should not be collinear and should agree with the general sense of rotation of wall edges. Edges may be cyclically interchanged in a wall list. The counting order  $w = 1, 2, 3, \dots$  of the walls is arbitrary.

Wall couples form a room wedge; they either have a (straight) real corner if the walls succeed each other, or they have a virtual corner if other walls are placed between the couple walls. The walls of a couple include a wedge angle  $\Theta$  (measured inside the room). Real corners are “concave” when  $0 < \Theta \leq \pi$  and “convex” for  $\pi < \Theta \leq 2\pi$ .

The acoustic qualification of a wall will use its surface admittance  $G_w$ . The MS method applies to the acoustic qualification of a wall its reflection factor  $R_w(\theta)$ , which is the reflection factor for a plane wave with incidence under the polar angle  $\theta$  formed by the normal to the wall and the connection line of the MS with  $P$ .  $R_w(\theta)$  depends on that angle, and thereby on the position of  $P$ , as:

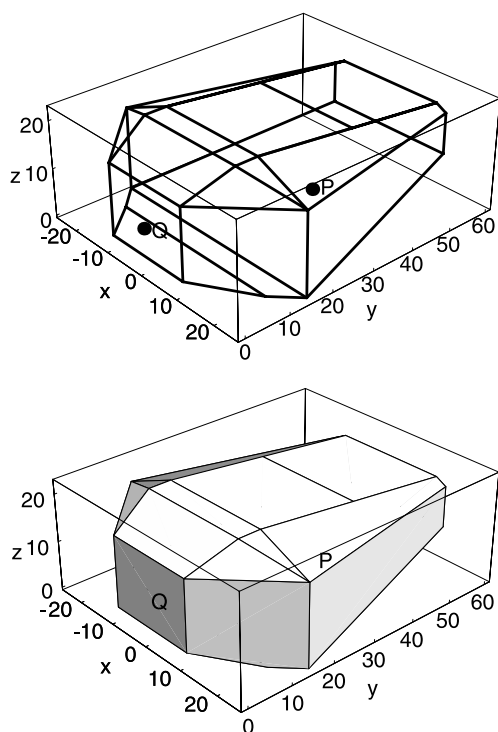
$$R_w(\theta) = \frac{\cos \theta - Z_0 G_w}{\cos \theta + Z_0 G_w}. \quad (4)$$

If the wall is bulk reacting, one further has  $G_w = G_w(\theta)$ .

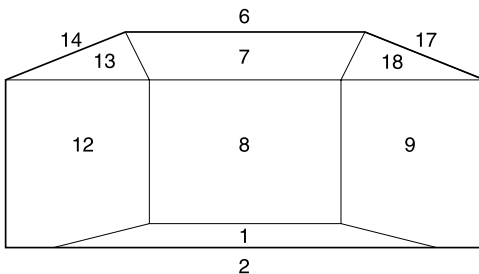
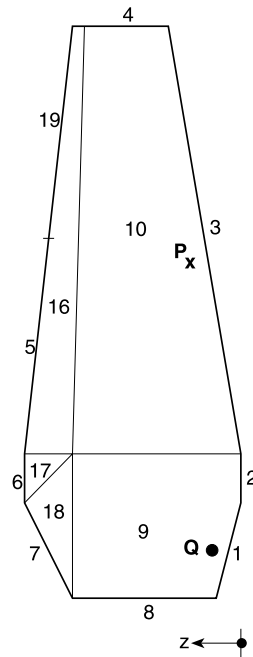
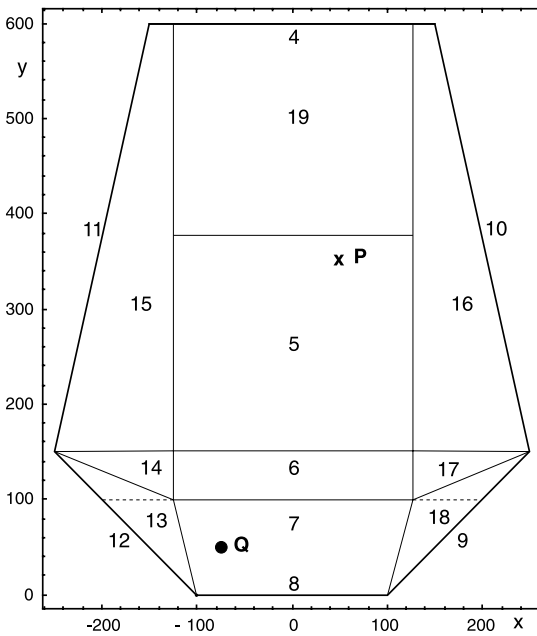
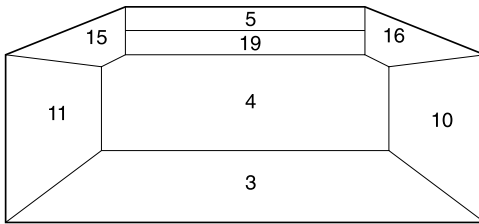
It is strongly recommended not to use too small parts of walls. Not only does the subdivision of the room envelope into too small wall sections produce analytical and numerical nonsense, but the computational work is increased immensely by the subsequent generation of MSs at such small faces. If one likes to consider the acoustic effect of e.g. pillars and/or handrails, it would be easier and faster to solve the task of scattering at suitable scatterers (e.g. cylinders or spheres). As a general rule for the dimensions of walls to be considered one can neglect walls with dimensions smaller than about  $\lambda_0$  (if the room itself is much larger than  $\lambda_0$ ).

### M.5.11 A Concave Model Room, as an Example

We consider a 3D model room which could function as a simple concert hall (see figures below). It has  $w = 1, 2, \dots, 19$  walls, two of them coplanar, and two couples have parallel walls on opposite sides of the room. The floors of the stage and of the seat area are inclined. Balconies cannot be modelled with concave rooms. The preceding 3D plots are computed from the input data (such plots are parts of the checks of input data). The first figure shows the room as a 3D wire plot, together with the source  $Q$  and the field point  $P$ ; the second figure shows an outside view of the room. The co-ordinate units are arbitrary.



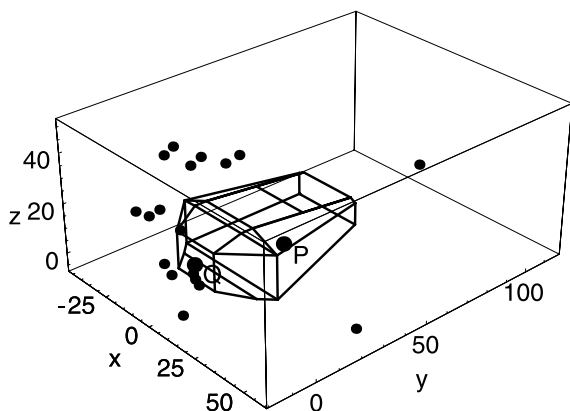
The enumeration of the walls ( $w = 1, 2, \dots, 19$ ), the plan and side elevations of the “concert hall”, the positions of source  $Q$  and receiver point  $P$ , are shown below in scaled co-ordinates:



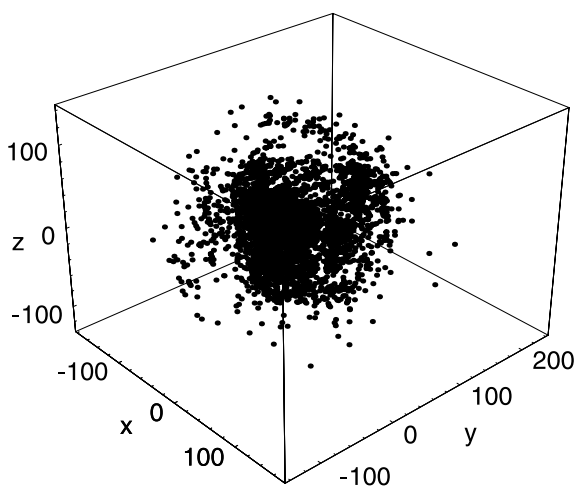
The normalised wall admittances  $Z_0 G_w$  for the example shown would produce a list of absorption coefficients  $\alpha_{\text{dif}}$  for diffuse sound incidence as given below for the list of the walls in the above enumeration. They are not exceptional in any sense.

$$\alpha_{\text{dif}} \approx \{0.10, 0.10, 0.40, 0.71, 0.20, 0.60, 0.20, 0.40, 0.20, 0.40, \\ 0.40, 0.20, 0.20, 0.20, 0.20, 0.20, 0.20, 0.20, 0.20, 0.50\}.$$

The following diagrams show MSs (as points) for two orders  $o = 1, 3$  if only back-reflection (into the position of the mother source) is avoided. Such diagrams would correspond to the mentioned numbers of MSs being claimed in the literature as “needed”.

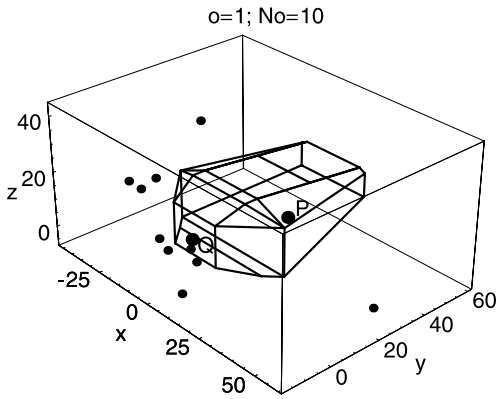


MSs of order  $o = 1$ , with only back-reflection criterion. Number of MSs: 19

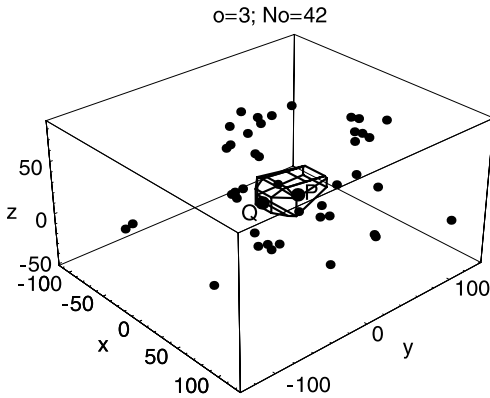


MSs of order  $o = 3$ , with only back-reflection criterion. Number of MSs: 6156

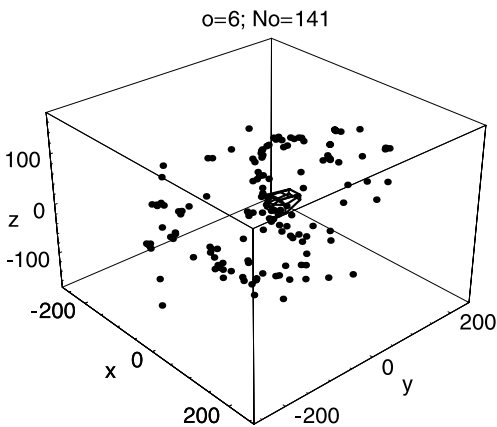
The next diagrams show the *effective* MSs with all interrupt criteria applied. In the test of exclusion of a wall as a mirror wall, it was checked whether the wall centre was inside the field angle cone of the mother source. It should be noticed that already for the order  $o = 1$  the number of MSs is reduced from 19 to 10 (mainly by the efficiency check).



Effective mirror sources of order  $o = 1$ , with all interrupt criteria. Number of MSs: 10



Effective mirror sources of order  $o = 3$ , with all interrupt criteria. Number of MSs: 42



Effective MSs of order  $o = 6$ , with all interrupt criteria. Number of MSs: 141

The published estimates  $n_w \cdot (n_w - 1)^{(o-1)}$  for the MSs of order  $o$  needed in a room with  $n_w$  walls would give for the order  $o = 6$  (with  $n_w = 19$  for our room) a number 35 901 792(!). The computing time for the effective MSs up to  $o = 6$  with all criteria of interrupt and effective source selection applied was 23 s (on an 800-MHz laptop computer with non-compiled Mathematica<sup>®</sup> programs).

The numbers of MSs in orders  $o$  for different applied criteria of interrupt are collected in the following Table 1.

**Table 1** Numbers of MSs in several orders  $o$  for different interrupt criteria applied

$o$	Back-reflection	& $q$ and wall inside	& effective
1	19	19	10
2	342	97	25
3	6256	261	42
4	110 808	478	69
5	1 994 544	755	99
6	35 901 792	1059	141

The next Table 2 collects, for each order  $o$ , minimum and maximum reductions in the level of the sound pressure contribution in  $P$  due to  $|IIR|$ , to  $\text{dist}(Q, P)/\text{dist}(q, P)$ , and to their product.

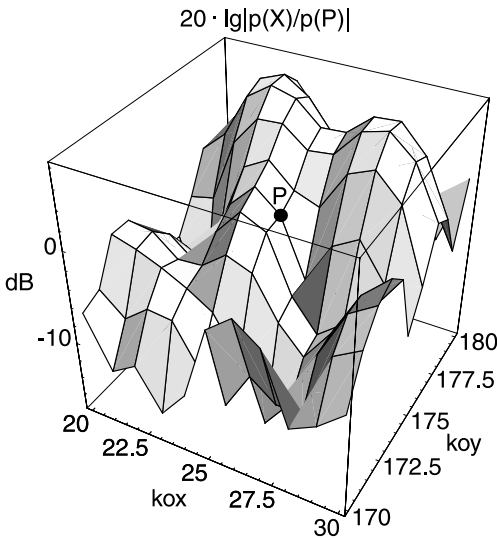
**Table 2** Minimum and maximum reductions in dB of level of field contributions in the order  $o$  by the source factor  $IIR$ , the distance ratio  $\text{dist}(Q, P)/\text{dist}(q, P)$ , and their product

$o$	$ IIR $		$\text{dist}(Q, P)/\text{dist}(q, P)$		$ IIR  \cdot \text{dist}(Q, P)/\text{dist}(q, P)$	
	min	max	min	max	min	max
1	7.34	0.566	4.69	0.122	7.46	0.948
2	21.05	1.32	10.23	0.331	25.57	4.36
3	22.61	1.69	14.2	4.36	32.29	6.93
4	22.96	3.06	15.91	4.86	36.02	8.89
5	36.21	3.58	18.86	7.34	49.29	12.86
6	37.72	4.19	19.01	8.98	52.91	14.53

The limits in the examples were set to  $|IIR| < 0.01 \sim -40$  dB;  $\text{dist}(q, P) > 10 \cdot \text{dist}(Q, P)$  (corresponding to  $-20$  dB of the distance ratio); so neither of the two limitations restricted the number of effective MSs. The table also shows that a limitation of the orders to  $o \leq o_{\max} = 6$  is reasonable because the highest contribution of a MS for  $o = 6$  is  $-14.53$  dB below the contribution of the original source  $Q$ .

As an example of application, we plot the profiles of the sound pressure level in places  $X = (x, y, z_p)$  around  $P = (x_p, y_p, z_p)$  as 3D plots of  $20 \cdot \lg|p(X)/p(P)|$  over  $k_0x$ ,  $k_0y$

for a fixed frequency. It is supposed that the distances  $\text{dist}(X, P)$  are small enough to neglect the influence of the variation of  $X$  on  $R(\theta_s)$ . (Such patterns cannot be computed with modified MS methods using  $|p_s(P)|$  or rays or sound particles as field descriptors because they lack phase.)



Profile of sound pressure level around  $P$ , for a higher frequency

### M.5.12 The MS Method in Rooms with Convex Corners

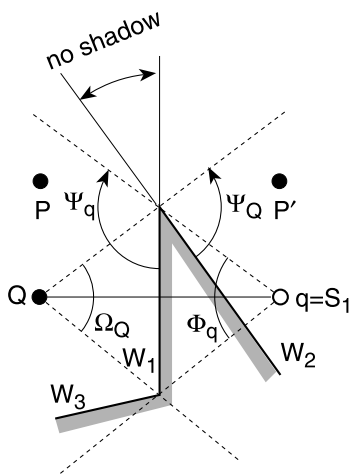
As shown above, the traditional MS method fails for the description of the sound field around convex corners (we shall solve this problem below). But one can apply the traditional form of the MS method in such rooms if one supposes that the scattered sound field in the shadow zone behind a convex corner can be neglected in comparison with the contributions of MSs which radiate into the shadow zone without scattering at the convex corner.

The mentioned supposition introduces the concept of “shading” into the MS method (see below). It is an important statement that a convex corner can be treated in the computations like a concave corner if the source  $q$  “sees” both flanks of the corner (from inside) because then no shadow is created. This condition is easily checked by “ $q$  inside both flanks”. The next figure shows a possible situation at a strongly convex corner in which the daughter source  $S_1$  of  $Q$  lies inside the room; this makes  $S_1$  illegal. Shading plays a role with a possible contribution of a source at  $P$  ( $P$  can be shaded or not), as well as with a possible continuation of MS production, if a wall is shaded.

$Q$  in the example below is ineffective if the field point is at  $P'$ ;  $P'$  is in the shade angle  $\Omega_Q$  which  $Q$  subtends with the wall  $W_1$ .

If we consider the MS  $q$ , it does not produce a daughter source at  $W_2$ , although it is inside that wall. Now  $\Phi_q$  is the field angle of  $q$  as defined and used in previous sections.



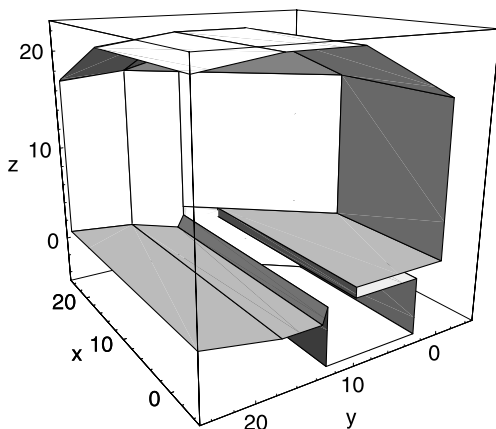


The requirement that  $q$  must not produce a daughter source at  $W_2$  is covered when we expand the condition for walls  $W$  at which a source  $q$  can produce a daughter source ( $W$  is inside  $\Phi_q$ ) by the additional requirement that  $W$  be inside the reflecting wall (here  $W_1$ ) as well

With that expanded rule,  $q$  can legally produce a daughter source at  $W_3$ .

The convex corner in the figure is treated like a concave corner if the source is in the range indicated with “no shadow”. This “no shadow” range gets larger for “mildly convex” corners. Thus the sound field evaluated in a room having only mildly convex corners will not be much different from the field in a similar room with only concave corners, as would be expected.

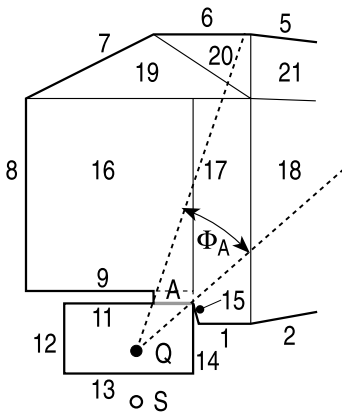
The situation is more complicated if two (or more) convex corners form an “aperture” which subdivides the room.



The picture shows, as an example, a 3D view from inside the room on the stage and into an orchestra pit (this model will be used later for application of the MS method).

The head of the stage and the balustrade of the orchestra pit form an aperture  $A$ .

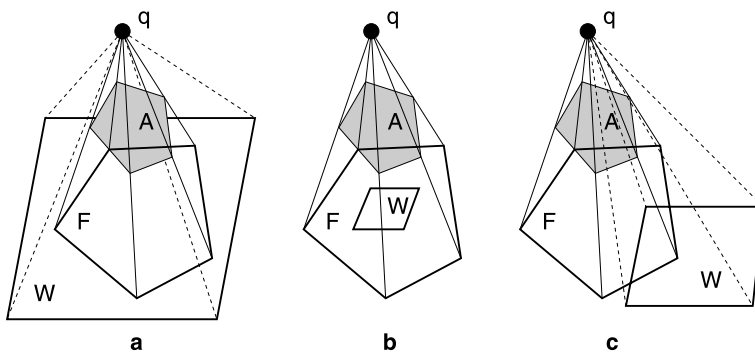
One must not only distinguish if the original source  $Q$  and the receiver  $P$  are on different sides of the aperture (for efficiency), but also a wall (for further MS production) must be seen by a source through the aperture, i.e. either  $P$  or a wall must be inside the aperture angle  $\Phi_A$  which is the cone subtended by the aperture  $A$  and with the source  $q$  in its apex.



Stage and orchestra pit from above (reversed side of view), with wall numbers and aperture angle  $\Phi_A$  subtended by the aperture  $A$ , and the source  $Q$

The “inside check” for  $P$  inside the cone( $q$ ,  $A$ ) is simple (see above). In concave rooms one can similarly test if a mirror wall is inside the field angle  $\Phi$  of a source by checking whether the wall centre is inside  $\Phi$ . This kind of check for the visibility of a wall through an aperture would be too inaccurate, however; important sound paths from one subspace (e.g. the orchestra pit) to the other subspace (e.g. the stage or the auditorium) could be missed with that kind of test.

The source  $q$  and the aperture  $A$  produce a “bright patch”  $F$  in the plane of an opposite wall  $W$  ( $F$  is the polygon formed in the plane of  $W$  by the intersection points  $X_i$  of the side corners of the cone( $q$ ,  $A$ ) with the plane of  $W$ ; they can be evaluated). Three cases of visibility should be distinguished; they are shown in the figure below.



One could describe the condition of visibility by the requirement that at least one edge of  $F$  is within  $W$  or at least one edge of  $W$  is within  $F$ . The implementation of this test would need the evaluation of the intersection points  $X_i$  and the test of whether a “point is within a polygon” (which should not be confused with “a point is inside the polygon plane”). One can avoid these (computer-intensive) subtasks by using the  $\text{cone}(q, W)$ . Then the visibility check reduces to the tests “at least one edge of  $A$  inside the  $\text{cone}(q, W)$ ” or “at least one edge of  $W$  inside the  $\text{cone}(q, A)$ ”.

The MS method in rooms with convex corners (in the supposed approximation which neglects corner scattering) has the same aim as in concave rooms, namely to find source lists  $\{q, w, \text{dist}(q, P), \text{IIR}, \text{flag}\}$  for legal sources  $q$ . As previously the frame program operates in three nested loops over the order  $o$ , the counting index  $s$  of the sources in the order  $o - 1$ , the counting index  $w$  of the walls. Because of the many decisions which must be made by the frame program anyway, it is advisable to write a subroutine for the MS evaluation, which is applicable for flanks of concave and convex corners, i.e. which internally only makes interrupt checks related to  $|\text{IIR}|$  and to  $\text{dist}(q, P)$  and efficiency tests for the new MS, whereas the frame program performs all interrupt tests. One can summarise the modifications of the MS method in rooms with convex corners as follows:

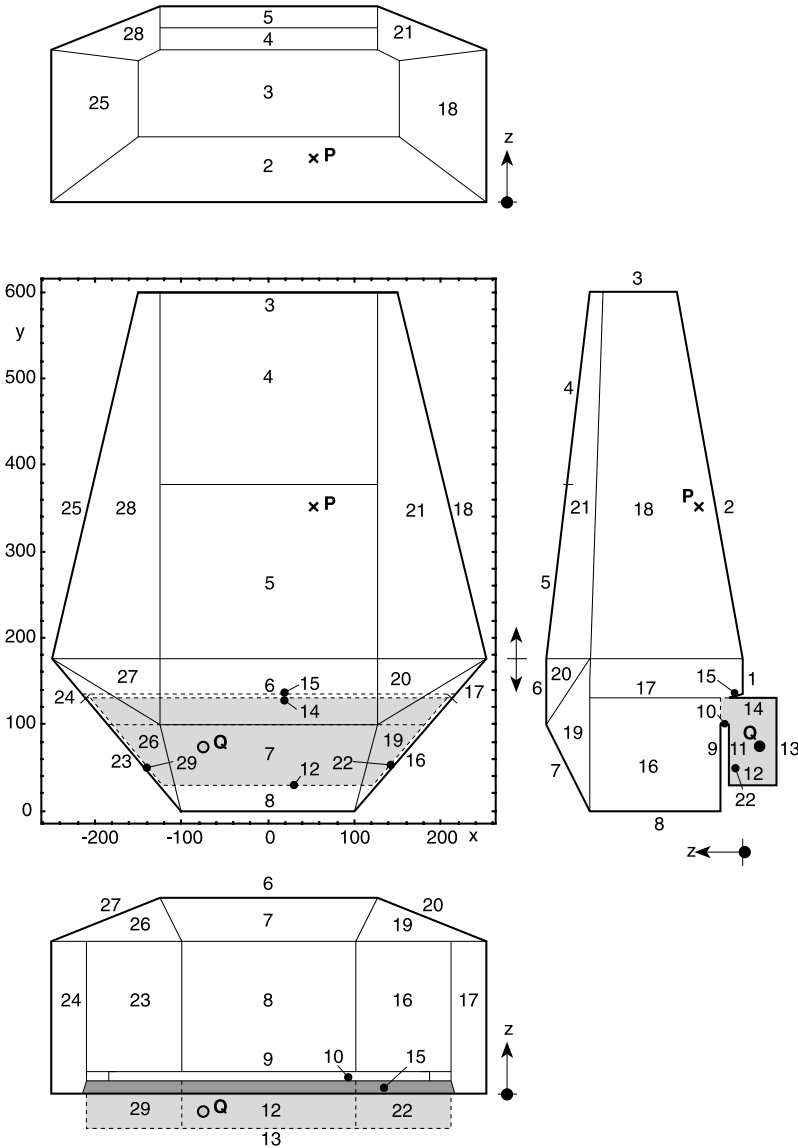
- 1) Find the lists of wall couples forming convex corners and of exclusive couples.
- 2) Determine the aperture  $A$  (if any).
- 3) An efficiency check must be performed already for the order  $o = 0$ , i.e. for  $q = Q$ . ( $Q$  is ineffective if  $P$  is on the other side of  $A$ , but not in  $\Phi_A$  of  $Q$ ; or, for a single convex corner when  $A$  is not defined, if  $P$  is in the shade angle  $\Omega_Q$  (a pyramid with  $Q$  at the apex and subtended by a wall  $W$  which is a flank of the convex corner)). Therefore determine  $\text{tabo}(0)$  in the frame program.
- 4) The source lists of the order  $o = 1$  (i.e. with  $Q$  as mother source) must also be determined separately in the frame program (because  $Q$  has no reflecting wall).
- 5) For orders  $o > 1$  the frame program in its innermost loop over the wall indices  $w$  has to check the interrupt conditions:
  - $w = w_m$ , the index of the reflecting wall;
  - the mother source  $q_m$  outside the wall with  $W(w)$ ;
  - for walls  $w, w_m$  on the same side of  $A$  if the centre of the wall  $w$  is outside the  $\text{cone}(q_m, W(w_m))$ ;
  - for walls  $w, w_m$  on different sides of  $A$ , if  $W(w)$  is not visible for  $q_m$  through  $A$ .
- 6) If none of the tests in 5) is positive, the frame program calls a subroutine for the evaluation of the source list of a new MS.

The subroutine causes an interruption (skip of  $w$ ) if  $|\text{IIR}| < \text{limit}$  or  $\text{dist}(q, P) > d_{\text{max}}$ . It also performs the efficiency tests. These efficiency checks are explained above.

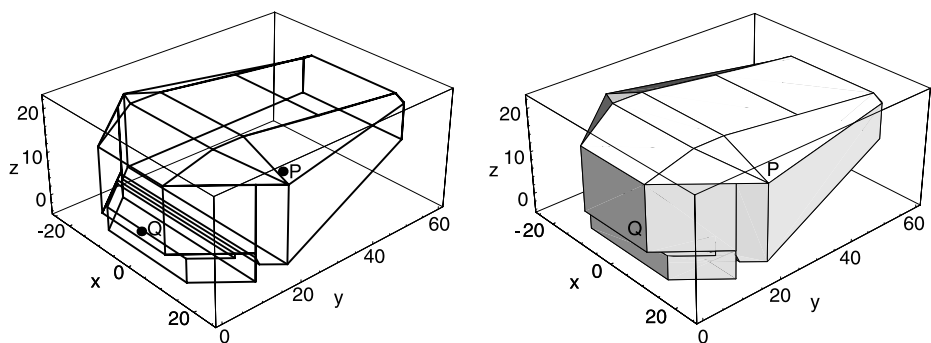
### M.5.13 A Model Room with Convex Corners

The model room of this section widely corresponds to the concave model room in the previous paragraph, but an orchestra pit is added below the stage (see the 3D view of the stage and the orchestra pit in the paragraph above; it shows a part of the present model room). A 3D wire plot of the walls and a 3D view from outside is shown in the next picture. The next page contains the plan and elevation views. The original source  $Q$  is placed in the orchestra pit; the receiving point  $P$  has the same position as in the previous

paragraph. The number of walls of the room is  $n_w = 29$ . There are three important convex corners: the upper corner of the balustrade at the orchestra pit and the upper and lower corners of the head of the stage floor.



Plan and elevation views of the “concert hall” with an orchestra pit, showing the enumeration of the walls,  $w = 1, 2, \dots, 29$ , and the positions of the source  $Q$  and of the receiver point  $P$  (scaling of the the co-ordinates different from the other graphs)



3D wire plot of a room, showing the positions of the source Q and of the field point P.

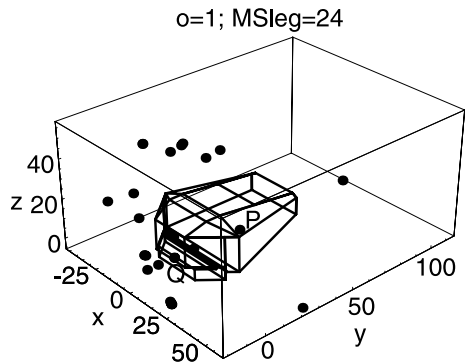
Table 3 gives the numbers of the legal and of the effective mirror sources in the orders  $o = 1, 2, \dots, o_{\max} = 6$ .

**Table 3** Number of legal and effective MSs of orders  $o = 1, 2, \dots, 6$

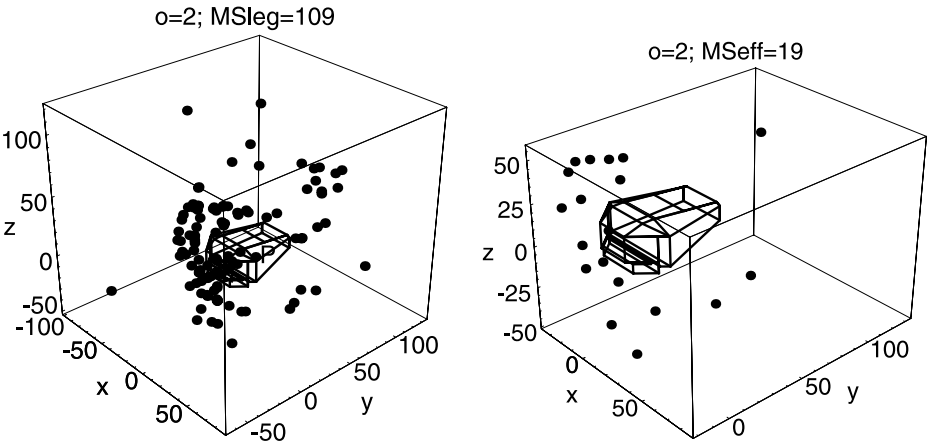
Type	$o = 1$	$o = 2$	$o = 3$	$o = 4$	$o = 5$	$o = 6$
Legal	24	109	286	637	1306	2467
Effective	0	19	44	96	186	272

All MSs of the order  $o = 1$  are ineffective, like the original source Q. The total number of effective sources is 617 up to  $o = 6$ ; the conventional prediction would require (with  $n_w = 29$ ) as the number of MSs:  $1 + \sum_{o=1}^6 n_w(n_w - 1)^{(o-1)} = 517\,585\,882$ .

The following diagrams show legal and effective MSs in 3D plots for some orders o (legal first, then effective, except for  $o = 1$ , where no effective MS exists).



Legal MSs with order  $o = 1$



Legal and effective mirror sources MS with order  $o = 2$  (pictures above) and  $o = 5$  (pictures below).

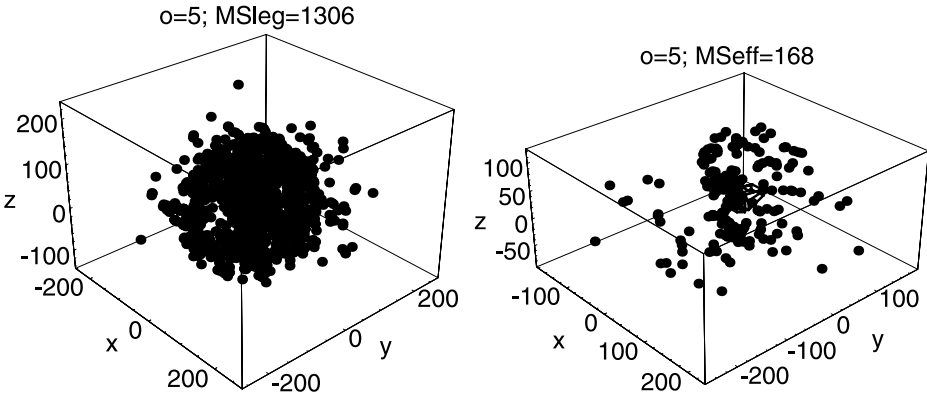
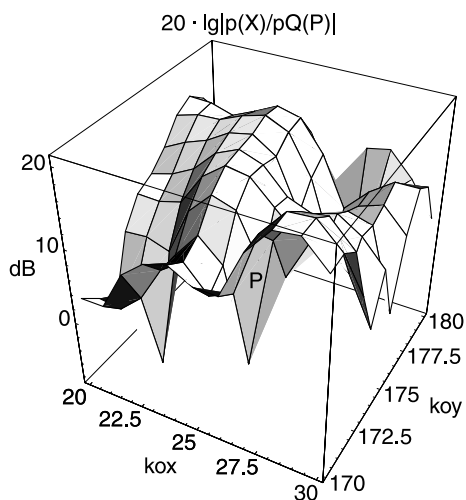


Table 4 presents the lowest values for the source factor  $|\Pi R|$  (in dB) and the lowest and highest values of  $|\Pi R| \cdot \text{dist}(Q, P)/\text{dist}(q/P)$  (in dB) within the listed orders. The table shows that, when using the product  $|\Pi R| \cdot \text{dist}(Q, P)/\text{dist}(q/P)$  as interrupt criterion, some MSs in the orders  $o = 5, 6$  could be dropped.

**Table 4** Level changes of contributions in the order  $o$

Level Change by	$o = 2$	$o = 3$	$o = 4$	$o = 5$	$o = 6$
$ \Pi R , \text{min}$	-4.38	-19.02	-23.81	-31.05	-34.59
$ \Pi R  \cdot \text{dist}(Q, P)/\text{dist}(q/P), \text{min}$	-12.37	-25.17	-30.88	-37.89	-47.13
$ \Pi R  \cdot \text{dist}(Q, P)/\text{dist}(q/P), \text{max}$	-3.37	-4.22	-3.38	-4.25	-6.98

Again, a final plot shows the sound pressure level profile around P (see previous paragraph for the assumptions made) and refers the level to the sound pressure which the free source Q would produce at P. The figure is for a higher frequency.



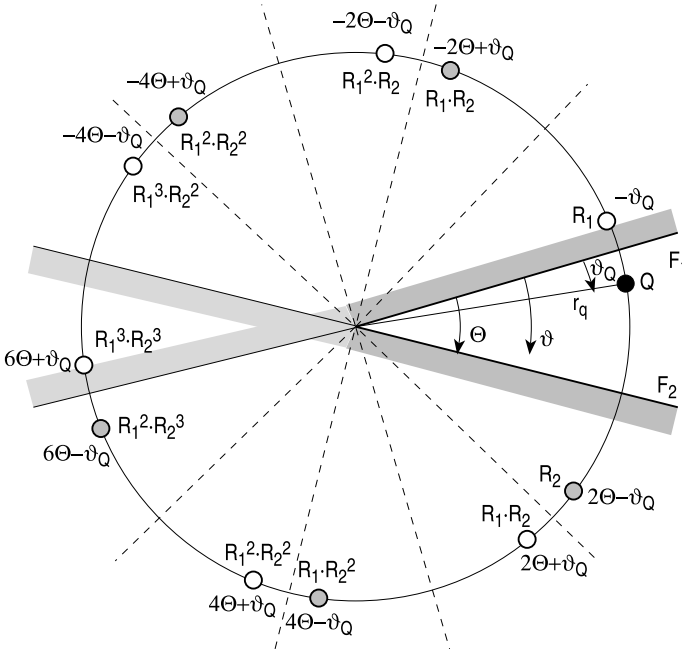
The contributions of the higher-order MSs lift the sound pressure level in the room significantly over the level in free space

### M.5.14 Other Grouping of Mirror Sources

This section is based on the easily proven fact that the original source Q and all MSs which are created by it and its daughter sources at a couple of walls  $F_1, F_2$  are arranged on a circle (“MS circle”) which contains Q and has its centre in the foot point Z of Q (normal projection) on the intersection line of the walls. So we are dealing with flanks of a corner; the corner is “real” if the flanks are subsequent walls of the room or “virtual” if other walls are arranged between the flanks. The corners (either real or virtual) may be concave or convex, but for the moment we consider only *concave corners*. A special case form antiparallel flanks: their (necessarily virtual) corner line is at infinity; the MS circle then becomes a straight line through Q normal to the flanks.

Because the plane containing the MS circle is normal to the flank corner, we are dealing with a two-dimensional problem (which is a further advantage of grouping the mirror sources in groups of MSs at wall couples). This suggests that the problem should be discussed within the context of a cylindrical co-ordinate system  $r, \vartheta$  centred at Z and with the reference for  $\vartheta$  preferably (but not necessarily) in one of the flanks. The radius of the MS circle will be symbolised by  $r_q$  and the angle for Q by  $\vartheta_Q$ , whereas the angle for a MS will be called  $\vartheta_q$ . The co-ordinates of the field point P are  $r, \vartheta, \zeta$ , where  $\zeta$  is the co-ordinate along the corner line, with  $\zeta = 0$  for Z, Q, q. The transformation between the Cartesian co-ordinates  $x, y, z$  of the room and the cylindrical co-ordinates  $r, \vartheta, \zeta$  of a flank couple is described in the appendix.

The next figure shows a couple of flanks  $F_1, F_2$ , the original source  $Q$  and its mirror sources on the MS circle.



The figure shows all legal MSs (the number is rather high because the wedge angle  $\Theta$  is small, by intention). The source at  $6\Theta - \vartheta_Q$  formally could be mirror-reflected once again, but then the daughter source would coincide with the MS at  $6\Theta + \vartheta_Q$  with the same source factor, so by the coincidence criterion this daughter source would be illegal. The indicated source factors as products of  $R_1, R_2$  should not be interpreted too literally; the factors in the powers of these reflection factors may contain different angles  $\theta_s$ .

The MSs on both circular arcs  $\vartheta < 0$  and  $\vartheta > 0$  have source angles  $\vartheta_Q$  within the limits:

$$\Theta - \pi < \vartheta_Q = -2s \cdot \Theta \pm \vartheta_Q < -\pi; \quad s = 0, \pm 1, \pm 2, \dots \quad (5)$$

The mirror sources lastly were generated at  $F_1$  for  $s < 0$ ; they would produce a daughter source on the lower circular arc with  $F_2$  if that is not excluded by the inside criterion, and vice versa for  $s > 0$ .

The range (Eq. M.5.(5))<sup>\*)</sup> leads to limits for the counter  $s$ :

$$\text{on the upper arc } \vartheta < 0: \quad 0 \geq s' > \frac{1}{2} \left( \frac{\pi \pm \vartheta_Q}{\Theta} - 1 \right); \quad (6a)$$

$$\text{on the lower arc } \vartheta > 0: \quad 0 < s < \frac{\pi \mp \vartheta_Q}{2\Theta}. \quad (6b)$$

$$\text{The sum of the counters is restricted to } s + |s'| < \frac{\pi}{\Theta} - \frac{1}{2}. \quad (7)$$

<sup>\*)</sup> See Preface to the 2<sup>nd</sup> edition.



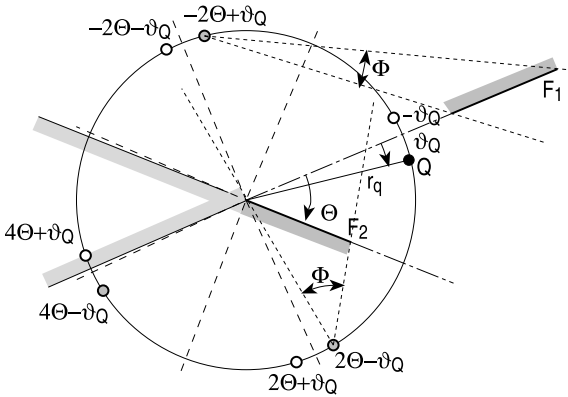
Thus the number of MSs decreases with increasing  $\Theta$ . If  $\Theta = \pi$ , then only the MS with  $n = 0$  is legal. Evidently, anti-parallel wall couples with  $\Theta = 0$  are a special case, which will be discussed separately below.

One needs, for the implementation of the MS method, the distance between  $q$  and  $P$  and the angle  $\theta_s$  formed by the connection line ( $q, P$ ) with the normal of the flank.

The distance between  $q$  and  $P$  is:  $\text{dist}(q, P) = \sqrt{\zeta^2 + r^2 + r_q^2 - 2r r_q \cos(\vartheta - \vartheta_q)}$ . (8)

The cosine  $\cos(\theta_s)$  is easily evaluated in the Cartesian co-ordinates, but this would need a co-ordinate transformation for all  $q$ . It is better to use the cylindrical co-ordinates of  $P$  and to evaluate  $\cos(\theta_s)$  in that system. This task will be described in the appendix.

The advantages of the described grouping are evident: one need not find the MSs by trial and error; they are evaluated in a straightforward method if the flanks have a real corner (where exclusion by interrupt and efficiency checks play no role). Further, one is sure to have covered all MSs for a wall couple. The question is whether one possibly introduces too many MSs if the flanks have a virtual corner. See the next figure for that question.



This graph illustrates the case that both flanks  $F_1, F_2$  are on different sides of the MS circle. The last MSs generated at the outer flank  $F_1$  never “see” the other flank  $F_2$ , and the last MSs generated at  $F_2$  may or may not have  $F_1$  in their field angles  $\Phi$ .

Conclusion: for flanks with a virtual corner the tests “ $F_i$  in cone( $q, F_j$ )” must be made as interrupt checks, except in situations which can be described and programmed easily in which the number of these tests can be reduced. Similarly, not only are the efficiency checks, which ask whether the projection  $P'$  of  $P$  into the plane of the MS circle is in the angle  $\Phi$ , simplified as compared to the traditional MS construction because this check now is a 2D check, but also conditions which make such checks unnecessary can be formulated. The tests “ $F_i$  in cone( $q, F_j$ )” remain three-dimensional if the flanking walls have a virtual corner and no intersection with the MS circle.

The set of mirror sources constructed in this way (we call it “corner set”) is “complete”; the sum of their contributions to  $p(P)$  is a precise field description (with the principal limitation of precision of the MS method) if only the flanking walls of the couple exist. We

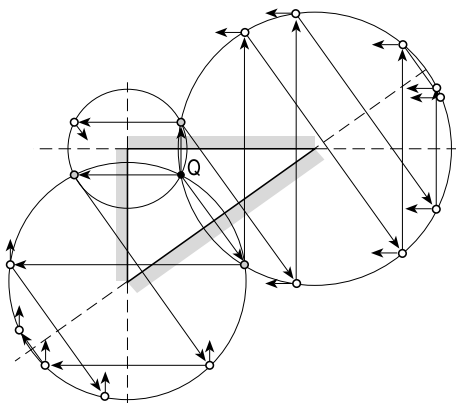
call their sound field the “corner field”. If  $P$  lies in between the flanks, it is plausible that this field represents the most important contributions of wall reflections at  $P$ . Further contributions come from other wall couples and their corner sets if  $P$  is in the field angle  $\Psi$  of those couples (see below) and by reflections of the corner set of a wall couple at other walls within  $\Psi$ . The combination of corner sets to the ensemble of mirror sources of a room (“room set”), or the completion of corner fields to the room field, will be discussed in the next paragraph.

### M.5.15 Combination of Corner Fields to Obtain the Room Field

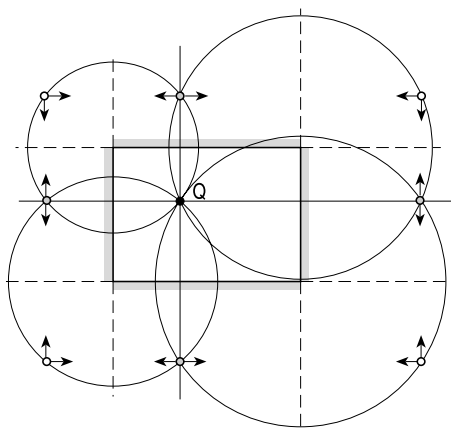
The room may have  $n_w$  walls  $W$ . Find solutions for corners with couples  $W_i, W_j$ ;  $i, j = 1, 2, \dots, n_w$ ;  $i \neq j$ ; that is  $n_w \cdot (n_w - 1)/2$  combinations (the combination  $W_i, W_j$  is equivalent to the combination  $W_j, W_i$ ).

For the preparation of the next idea we take the simplest examples of two-dimensional triangular and rectangular rooms. If the room has a 3D tetrahedral shape, for example, the main difference as compared to a two-dimensional room would be an inclination of the MS circles relative to each other (it is simpler to compute the situation in a 3D room than to present it in a graph). Below, MSs from the traditional MS method are drawn with interrupts according to the inside criterion. This will be sufficient for the ensuing argumentation.

The MSs created at a wall couple are collected on circles. In the next figure for a triangular room, three of the MSs appear twice (they are marked with a grey fill); they are the MSs of first order. In the subsequent figure for a rectangular room the vertical and horizontal lines through  $Q$  represent the limit cases of MS circles for the two antiparallel wall couples. In that figure the four MSs of the first order appear three times. Long arrows in the figures indicate where the MSs come from. Short arrows indicate at which wall the MSs shown should be mirror-reflected in the next step of MS production. These arrows point to opposite walls.



The original source  $Q$  appears three times in the three corner sets; the MSs of first order appear twice.



The original source  $Q$  appears four times in the four corner sets; the MSs of the first order appear three times.

The facts that the MSs of a wall couple are placed on a circle around the wall corner with  $Q$  on the circle, and that the continuation of MS production would imply opposite walls, suggest that one should collect the MSs of a wall couple into one equivalent source for the corner field. The following rules are evident from the above discussion:

- exclude the original source from the field of that source;
- exclude the MSs of the first order from that source;
- define the field angle  $\Psi$  of the source.

We shall see in the next section that the new source is placed in the foot point  $Z$  of  $Q$  on the corner line. The field angle  $\Psi$  therefore is the angle defined by the two flanks and the corner line as apex line.

### M.5.16 Collection of the MSs of a Wall Couple in a Corner Source

Up to now the graphs in the previous paragraph indicate nothing more than an involved, but legitimate, procedure of traditional MS production; only the collection of the MSs is special.

Now we take advantage of the fact that the MSs of a wall couple are arranged on a circle around the intersection line (normal to that line) which also contains  $Q$  (and thereby defines the radius  $r_q$  of the circle). The intersection line between the walls must not really exist (see the rectangular room above). But first we exclude the special case of parallel walls (it will be treated below as a special case). Let the radius of the MS circle be designated as  $r_q$ .

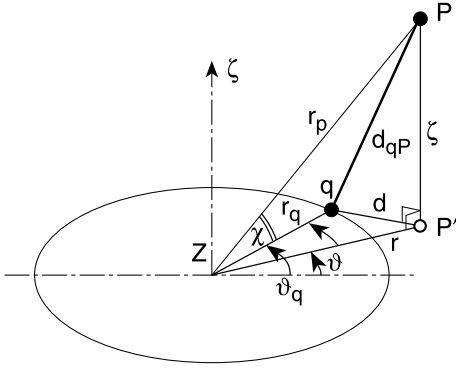
The field of a MS at  $P$  is described by:

$$\begin{aligned}
 p_q(P) &= \Pi R \cdot h_0^{(2)}(k_0 d_{qp}) = \frac{\Pi R}{k_0 d_{qp}} \cdot [\sin(k_0 d_{qp}) + j \cos(k_0 d_{qp})] \\
 &= j \Pi R \frac{e^{-jk_0 d_{qp}}}{k_0 d_{qp}}
 \end{aligned} \tag{9}$$

with  $d_{qp} = \text{dist}(q, P)$ . The addition theorem for spherical Bessel functions, when applied to the above expression, leads to:

$$h_0^{(2)}(k_0 d_{qp}) = \sum_{n \geq 0} (2n+1) \cdot P_n \left( \frac{r}{r_p} \cos(\vartheta_q - \vartheta) \right) \cdot \begin{cases} j_n(k_0 r_p) \cdot h_n^{(2)}(k_0 r_q); & r_p < r_q \\ j_n(k_0 r_q) \cdot h_n^{(2)}(k_0 r_p); & r_p > r_q \end{cases}, \quad (10)$$

where  $j_n(x)$  are spherical Bessel functions of order  $n$ ,  $h_n^{(2)}(x)$  are spherical Hankel functions of the second kind,  $P_n(x)$  are Legendre polynomials, and the geometrical quantities are taken from the next figure.



The *circle* is the MS circle;  $q$  is a source on it with the cylindrical co-ordinates  $r_q, \vartheta_q, \zeta = 0$ ;  $P$  is the field point with the cylindrical co-ordinates  $r, \vartheta, \zeta$ ;  $P'$  is the projection of  $P$  on the plane of the MS circle.

The following relations exist among the geometrical quantities:

$$d_{qp}^2 = r_q^2 + r_p^2 - 2r_q r_p \cos \chi, \quad (11)$$

$$r_p^2 = r^2 + \zeta^2,$$

$$d_{qp}^2 = d^2 + \zeta^2, \quad (12)$$

$$d^2 = r_q^2 + r^2 - 2r_q r \cos(\vartheta_q - \vartheta),$$

from which it follows that:

$$\cos \chi = \frac{r}{r_p} \cos(\vartheta_q - \vartheta). \quad (13)$$

The first line in Eq. M.5.(11) was used for the addition theorem.

Summation over the sources on the MS circle gives for the field contribution at  $P$  of that sources:

$$p(P) = j \sum_s \Pi_s R(\theta_s) \sum_{n \geq 0} (2n+1) \cdot P_n \left( \frac{r}{r_p} \cos(\vartheta_{qs} - \vartheta) \right) \cdot \begin{cases} j_n(k_0 r_p) \cdot h_n^{(2)}(k_0 r_q); & r_p < r_q \\ j_n(k_0 r_q) \cdot h_n^{(2)}(k_0 r_p); & r_p > r_q \end{cases}. \quad (14)$$

The summation index  $s$  can be taken from Eq. M.5.(5) if all sources are added. As explained above, it is recommended that one avoid the summation over  $Q$  and the MSs of the first order (their field contributions will be added to the field in their traditional forms); and illegal or inefficient sources will also be left out of the summation over  $s$ . Eq. M.5.(14) represents an important group of mirror sources in an explicit formula. The terms represent radially standing waves in  $r_p$  if  $r_p < r_q$  and outward propagating waves if  $r_p > r_q$ . The sound field is continuous at  $r_p = r_q$ . The sum satisfies the boundary conditions at the flanks, Sommerfeld's far field condition, the source condition and the edge condition (which requires that the volume flow through a small cylinder around a corner or a sphere around an edge does not exceed the volume flow through a similar cylinder or sphere, respectively, around the original source  $Q$ ; the edge condition mostly is used for the selection of permitted radial functions, like Sommerfeld's far field condition). But Eq. M.5.(14) in general does not satisfy the wave equation because the factors  $\Pi_s(\theta_s)$  in general are neither constant nor do they have the form required by the wave equation for angular factors to Bessel functions of order  $n$ . However, satisfaction of the wave equation could not be expected with the MS method as a basis for Eq. M.5.(14).

This representation, however, has a numerical problem: the convergence and the precision are critical for  $r_p = r_q$ , i.e., if the field point lies on the sphere which has the MS circle as equator circle. Physically the numerical problem comes from the fact that the sphere surface contains the poles of the sources  $q$ . The evaluation of Eq. M.5.(14) at  $r_p = r_q$  needs a careful check of the summation limit for  $n$  (a detailed discussion of the convergence check can be found in Mechel (2002)). This problem in general does not appear after a mirror-reflection of Eq. M.5.(14) at an opposite wall (see below). One could avoid it by using the traditional MS method at or near  $r_p = r_q$ , but this would require the programming of both methods. An easier method in the case  $r_p = r_q$  is the evaluation of Eq. M.5.(14) on both sides of that limit, at some distance, and then to take the mean value.

The fact that a set of spherical Bessel and Hankel functions with integer orders must be evaluated causes no problem; the set can be obtained from two start values of the order by the known recursions of such functions, and also the Legendre polynomials are easily computed. The radial arguments are constant for all sources on the MS circle and for a fixed immission point  $P$ .

Important conclusions can be drawn from Eq. M.5.(14). The components of the sum over  $n$  are spherical wave terms, which are centred at the centre  $Z$  of the MS circle on the corner line. Therefore we say that Eq. M.5.(14) represents the field of a "corner source". It can be introduced into a continued MS generation like any directional source. The advantages of the corner source are evident. Its position need not be found in a complicated search algorithm; it is explicitly defined by the room geometry and the position of  $Q$ . Also, its field angle  $\Psi$  is immediately given; it is the angle between the flanking walls. The difference with the field angle  $\Phi$  of a traditional MS is remarkable ( $\Phi$  is the angle of the cone subtended by the reflecting wall and the MS in the apex). Efficiency checks ( $P$  in  $\Psi$ ?) and interrupt checks (an opposite wall in  $\Psi$ ?) are much easier to perform.

It is not proven, but plausible, that one can stop the field evaluation after the corner sources of all wall couples have been evaluated and mirror-reflected once at their op-

posite (visible) walls. All really important field contributions will be obtained with that procedure.

The mirror reflection of the corner source is done by a simple modification of Eq. M.5.(14) if one applies the reciprocity of the next paragraph. One must not evaluate the positions of the mirror-reflected sources, but one mirror-reflects  $P$ , multiplies the  $IIR(\theta_s)$  in the sum over  $s$  by the new reflection factor, and evaluates Eq. M.5.(14) with the geometrical parameters of the new position of  $P$  (which can also be determined directly from the room input data and the position of  $P$ ). This procedure avoids the reflection of the directivity of the corner source.

### M.5.17 A Kind of Reciprocity in the MS Method

Evidently, a source  $q$  generated by a mother source  $q_m$  at a mirror wall  $W$  will produce at a receiver point  $P$  the same contribution  $p(P)$  that the mother source  $q_m$  would produce at the point  $P'$ , which is the mirror-reflected point to  $P$  with respect to  $W$ , after multiplication by  $R(\theta_s)$ .

So one could set up a “mirror-receiver method” instead of a “mirror-source method” by recasting all interrupt and efficiency rules. Numerically there would be no advantage as compared with the MS method for isotropic sources  $Q$ . If, however, the original source  $Q$  has a directivity  $D(\vartheta, \varphi)$ , the mirror-receiver method avoids the mirror reflection of the directivity.

### M.5.18 Limit Case of Parallel Walls

Because only antiparallel walls will be considered here, we use the abbreviation “parallel” walls. In principle, the number of MSs needed for the sound field in the space between parallel walls is infinitely high (on both sides of the walls). Up to now we have had only an interrupt criterion if the walls are absorbent due to the reduction of the source factor  $IIR$  with increasing order.

In the limit case of parallel walls in Eq. M.5.(14) the limits  $r, r_p, r_q \rightarrow \infty$  and  $\vartheta \rightarrow 0$  are assumed; the MS circle becomes a straight line normal to the walls.

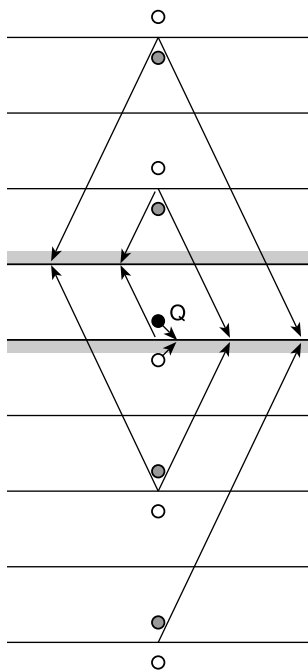
First we derive with the next figure a plausible interrupt criterion for the MS production with parallel walls by consideration of allowable errors; then we sum up the MSs to a single equivalent source.

The *arrows* indicate which couples of sources satisfy the boundary condition at which wall.

After an interrupt one has a couple without a “partner” for the boundary condition (this is the lowest couple in the graph). An interruption makes an error in the boundary condition at a wall. The absolute error is in the order of magnitude of the field contribution of the uncompensated couple.

It decreases with increasing order of reflection

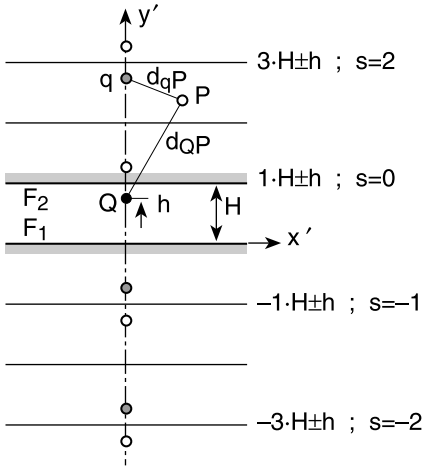
- because of the increasing distance of the couple to the wall (geometrical reduction),
- because of the decrease of  $IIR$  with absorbent walls (acoustical reduction).



The relative error, which is important, further decreases with increasing order because the reference quantity is the sum of contributions of “complete” couples.

From experiences of field evaluations in flat ducts (which, indeed, is the object at hand) one can conclude that a relative boundary value error  $\Delta_{\text{rel}} \approx 1/10$  to  $1/20$  is tolerable. Neglecting geometrical and acoustical reductions, this leads to a permitted interrupt at about  $s_{\text{hi}} = 10$  to  $20$  MSs. This will be sufficient if geometrical reduction with increasing order is taken into account and if one considers that real walls never are ideally reflecting. A reflection coefficient  $|R| = 0.9$  produces for an order  $o = 15$  a source factor of about  $0.9^{15} = 0.206$ .

One can perform an analysis as in ► *Sect. M.5.15* for parallel walls as well. Its principal result is a recommendation to write the sound field of the MS for parallel walls as the field of the original source multiplied by a directional factor. But, knowing this goal, it is easier to derive that form of the MS field directly. The problem is characterised geometrically by the straight line, normal to the flanks  $F_1, F_2$ , which contains the original source  $Q$  and the MS  $q$ , and the field point  $P$ . We therefore take a right-handed Cartesian co-ordinate system  $x', y', z'$  with the  $y'$  axis on the source line and the  $x'$  axis in one of the flanks so that  $P$  is in the  $x', y'$  plane (it follows from the system  $x, y, z$  of the room by a rotation and shift); see next figure.



The source positions are given by  $x' = 0, z' = 0$  and

$$x'_q = (2s + 1) \cdot H \pm h; \quad s = 0, \pm 1, \pm 2, \dots, \quad (15a)$$

if the co-ordinate origin is chosen on  $F_1$  as in the figure, otherwise by

$$x'_q = 2s \cdot H \pm h; \quad s = 0, \pm 1, \pm 2, \dots \quad (15b)$$

The field contribution  $p_q(P)$  at  $P$  of a source  $q$  can be written in terms of the contribution  $p_Q(P)$  of  $Q$  as:

$$p_q(P) = \Pi_q R(\theta_s) \cdot \frac{k_0 d_{QP}}{k_0 d_{qP}} e^{-jk_0(d_{qP} - d_{QP})} \cdot p_Q(P) \quad (16)$$

with

$$d_{qP} = \sqrt{(x'_p - x'_q)^2 + (y'_p - y'_q)^2}; \quad d_{QP} = \sqrt{(x'_p - x'_Q)^2 + (y'_p - y'_Q)^2}. \quad (17)$$

The angles  $\theta_s$  for the reflection factors are easily obtained in the  $x', y'$  co-ordinates. The equivalent source and its contribution representing all mirror sources are given by:

$$p(P) = p_Q(P) \sum_s \Pi_q R(\theta_s) \cdot \frac{k_0 d_{QP}}{k_0 d_{qP}} e^{-jk_0(d_{qP} - d_{QP})}. \quad (18)$$

For the combination with corner sources of non-parallel wall couples it is again recommended to leave the original source and the MSs of the first order out of the summation over  $s$ . For the mirror reflection of this source at an opposite wall use the reciprocity, i.e. determine the position of the reflected field point  $P'$  in the co-ordinates  $x', y', z'$ .

If the parallel flanks  $F_1, F_2$  are not directly opposite to each other, but with a parallel offset, interrupt checks for mirror sources are preferably performed in the co-ordinates  $x', y', z'$  (skip  $s$  for illegal sources in Eq. M.5.(18)), as well as efficiency checks (skip  $s$  for inefficient sources). The total source Eq. M.5.(18) is ineffective if  $P$  is not in the space between the planes of the flanks  $F_1, F_2$ , and the mirror-reflected combined source is



ineffective if  $P'$  is not in that space. So indeed one has to form two sums as in Eq. M.5.(18), one for the “legal” equivalent source, which is used in its mirror reflection, and one for the final evaluation of the field contribution. But the decision about whether Eq. M.5.(18) must be evaluated at all can be made before any computation.

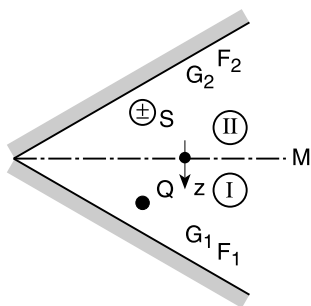
One still has the problem with convex corners and their scattered field. This problem can be solved rather easily, within the frame of a MS method, by combination of the MS method with the “second principle of superposition” (PSP). See ➤ Sect. B.10 for that principle. It will be briefly repeated below because it will take special forms in combination with the MS method.

### M.5.19 The Second Principle of Superposition (PSP)

It should be stated in advance:

- The PSP, when applied to single concave corners, does not result in significant computational savings as compared to the traditional MS method;
- unless it is globally applied to symmetrical rooms (see below);
- but its application is necessary with convex corners;
- because it is applicable to both convex and concave corners, and some of its features are more easily explained with concave corners, these are treated here also.

The objects of the second PSP are an arbitrary (also multimodal) source  $Q$  and a scattering object which has a plane of symmetry  $M$ . When the PSP is applied to room edges, the flanking walls are assumed to extend from their line of intersection to infinity. If they are absorbent, the absorption should be the same at both flanks (symmetrical flanks; see below for unsymmetrical flanks). It is not necessary that the flanking walls of a room have a real line of intersection; they may be couples of walls, with other walls between them on the apex side.



We assume equal wall admittance values  $G_i$  at both flanks  $F_i$ . We further assume a co-ordinate system with a co-ordinate  $z$  (which preferably is an azimuthal co-ordinate) normal to the median plane  $M$ . This assumption is not necessary; it just simplifies the description.

The median plane  $M$  subdivides the wedge into two halves:

- (I) on the source side of  $M$ ,
- (II) on the back side of  $M$  (as seen from  $Q$ ).

With the above choice of  $z$ , mirror-reflected points in both halves are distinguished just by  $\pm z$ .

The PSP composes the solution of the original scattering task by the solutions of two subtasks  $\sigma = h, w$  of scattering in zone (I):

- in the first subtask,  $\sigma = h$ , the plane of symmetry  $M$  is assumed to be hard;
- in the second subtask,  $\sigma = w$ , the plane of symmetry  $M$  is assumed to be soft.

The field of each subtask is composed of the source field  $p_Q$  and a scattered field  $p_s^{(\sigma)}$ :  $p^{(\sigma)} = p_Q + p_s^{(\sigma)}$ . The fields of the original task in both zones (I) and (II) then are:

$$\begin{aligned} p_I(x, z) &= p_Q(x, z) + \frac{1}{2} (p_s^{(h)}(x, z) + p_s^{(w)}(x, z)) , \\ p_{II}(x, z) &= \frac{1}{2} (p_s^{(h)}(x, -z) - p_s^{(w)}(x, -z)) \end{aligned} \quad (19a)$$

( $x$  represents the co-ordinates other than  $z$ ). One can also decompose the field as  $p^{(\sigma)} = p_Q + p_r + p_s^{(\sigma)}$ , where  $p_r$  is the same in both subtasks; then we have:

$$\begin{aligned} p_I(x, z) &= p_Q(x, z) + p_r(x, z) + \frac{1}{2} (p_s^{(h)}(x, z) + p_s^{(w)}(x, z)) , \\ p_{II}(x, z) &= \frac{1}{2} (p_s^{(h)}(x, -z) - p_s^{(w)}(x, -z)) . \end{aligned} \quad (19b)$$

The scattered fields here are generally different from those of Eq. M.5.(19a), but in our problem  $p_r$  is just a member of the scattered field terms (see below), so that these remain unchanged.

In summary: the PSP solves the scattering task on the source side (I) for the subtasks  $\sigma = h, w$  and computes with them the field on the back side (II) (by simple mirror reflection at  $M$ ). One should keep in mind this “detour” of the field evaluation in (II) via zone (I).

The *derivation* of the PSP uses, in addition to the source  $Q(x, z)$ , sources  $Q(x, -z)$ , which are mirror-reflected at  $M$ ; in the first subtask the MS has the same amplitude as  $Q$ ; in the second subtask it is multiplied by  $-1$ . Equations M.5.(19a) just describe the superposition of both subtasks with  $Q$  and  $\pm MS$  as sources. The following features should be observed:

- The simplicity of the derivation shows the general validity of the PSP (under the mentioned condition of object symmetry).
- The PSP is an exact description if the scattered fields of the subtasks can be determined exactly.
- The PSP is suitable for combination with the MS method!
- If, in the course of applying the PSP, mirror sources are created at  $M$  (to satisfy the boundary conditions there), one should remember that mirror sources at ideally reflecting planes give an exact description of the field. With absorbing flanks, the errors of the MS method remain.
- The fields of the mirror sources  $S_i$  form the “scattered fields”. If  $S_i$  is created by mirror reflection at  $F_1$  on the source side, the sign of the MS is the same in both subtasks; this will be indicated in the sketches below with (+). If  $S_i$  is created by

mirror reflection at M, the sign of  $S_i$  is different in both subtasks; this will be marked in the sketches with  $(\pm)$ , i.e.  $(+)$  for  $\sigma = h$ ,  $(-)$  for  $\sigma = w$ . If a MS created at M (i.e. marked with  $(\pm)$ ) afterwards is reflected at  $F_1$ , the double sign  $(\pm)$  remains.

The resulting fields of the PSP are:

$$\begin{aligned} p_I(x, z) &= Q + \frac{1}{2} \left( \sum_i S_i^{(h)}(x, z) + \sum_i S_i^{(w)}(x, z) \right), \\ p_{II}(x, z) &= \frac{1}{2} \left( \sum_i S_i^{(h)}(x, -z) - \sum_i S_i^{(w)}(x, -z) \right). \end{aligned} \quad (20a)$$

The change  $h \rightarrow w$  of the median plane M does not influence the position and number of the MSs; therefore the sums have the same counting and summation index  $i$ .

If the first MS is created at  $F_1$  (on the source side), it has in both subtasks the same sign (it will be indicated by  $S_0$ ). In  $p_I(x, z)$  it can be pulled to outside the parentheses and needs no superscript (h) or (w). The remaining MSs under the sums (with superscripts) have undergone at least one mirror reflection at M. Thus one can write:

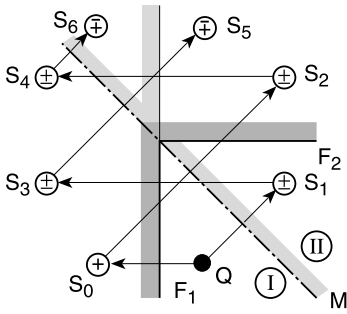
$$\begin{aligned} p_I(x, z) &= Q + S_0(x, z) + \frac{1}{2} \left( \sum_i S_i^{(h)}(x, z) + \sum_i S_i^{(w)}(x, z) \right), \\ p_{II}(x, z) &= \frac{1}{2} \left( \sum_i S_i^{(h)}(x, -z) - \sum_i S_i^{(w)}(x, -z) \right). \end{aligned} \quad (20b)$$

With the production of MSs in the PSP one must distinguish the following:

- 1.) "Mirror reflected at..."
  - (a) the wall  $F_1$ ; then the sign is the same as for the mother source; if  $F_1$  is absorbent, a reflection factor  $R$  arises;
  - (b) at M, then the sign in the subtask  $h$  is that of the mother source; in the subtask  $w$  the sign is changed, i.e. the new factor in the source factor  $\Pi R$  is  $R = \pm 1$ .
- 2.) Two subtasks
  - (a)  $\sigma = h$ : no sign change at mirror reflections;
  - (b)  $\sigma = w$ : sign change for mirror reflections at M (but not at  $F_1$ ).
- 3.) Two "paths" of MS production:
  - (a) first path: begins with mirror reflection at  $F_1$ ;  
MSs on this path will be designated with even indices  $i = 0, 2, 4, \dots$ ;
  - (b) second path: begins with mirror reflection at M;  
MSs on this path will have odd indices  $i = 1, 3, 5, \dots$

Whereas the subtasks  $h, w$  do not change the position of a MS of some order, the positions of the MSs of both paths are generally different from each other.

As a detailed example we take the concave rectangular corner of the next figure.



Here the MS production is continued (irrespective of the inside criterion) until the MSs begin to fall on positions of previously created MSs. The paths from then on would begin to be followed backwards (with multiple covering of the positions).

The following schemes represent the chains with multiple reflections at  $F_1$  and  $M$  for both paths. Mirror reflection at  $F_1$  is marked by a simple arrow  $\rightarrow$  and reflection at  $M$  by a double arrow  $\Rightarrow$ . The cases  $\sigma = h$  are arranged in the upper line and  $\sigma = w$  in the lower line. MSs in vertical columns of the scheme have equal spatial positions. The flanking wall  $F_1$  is initially assumed to be rigid.

Under the symbols of the MSs in the schemes below are written the sums appearing in the PSP (for one path; recall that MSs in a column of the scheme have equal spatial positions):

$$\sum S = \sum_{i \geq 0} S_i^{(h)} + S_i^{(w)} \quad \text{in zone (I) ,}$$

$$\Delta S = \sum_{i \geq 0} S_i^{(h)} - S_i^{(w)} \quad \text{in zone (II).}$$

First path:

$$Q \xrightarrow{h} S_0 \xrightarrow{h} +S_2 \rightarrow +S_4 \Rightarrow +S_6 \rightarrow +S_8 \Rightarrow +S_{10} \rightarrow +S_{12}$$

$$Q \xrightarrow{w} S_0 \xrightarrow{w} -S_2 \rightarrow -S_4 \Rightarrow +S_6 \rightarrow +S_8 \Rightarrow -S_{10} \rightarrow -S_{12}$$

$$\sum S = \sum_{i \geq 0} S_i^{(h)} + S_i^{(w)} = 2S_0 \quad 0 \quad 0 \quad 2S_6 \quad 2S_8 \quad 0 \quad 0 \quad (21a)$$

$$\Delta S = \sum_{i \geq 0} S_i^{(h)} - S_i^{(w)} = 0 \quad 2S_2 \quad 2S_4 \quad 0 \quad 0 \quad 2S_{10} \quad 2S_{12}$$

Second path:

$$Q \xrightarrow{h} +S_1 \rightarrow +S_3 \Rightarrow +S_5 \rightarrow +S_7 \Rightarrow +S_9 \rightarrow +S_{11}$$

$$Q \xrightarrow{w} -S_1 \rightarrow -S_3 \Rightarrow +S_5 \rightarrow +S_7 \Rightarrow -S_9 \rightarrow -S_{11}$$

$$\sum S = \sum_{i \geq 0} S_i^{(h)} + S_i^{(w)} = 0 \quad 0 \quad 2S_5 \quad 2S_7 \quad 0 \quad 0 \quad (21b)$$

$$\Delta S = \sum_{i \geq 0} S_i^{(h)} - S_i^{(w)} = 2S_1 \quad 2S_3 \quad 0 \quad 0 \quad 2S_9 \quad 2S_{11}$$

If one sums up the MSs of both paths, the PSP gives:

$$\begin{aligned}
 p_I(x, z) &= Q(x, z) + S_0(x, z) + \sum_{n=1,3,5,\dots} \sum_{k=1}^4 S_{4n+k}(x, z), \\
 p_{II}(x, z) &= \sum_{n=0,2,4,\dots} \sum_{k=1}^4 S_{4n+k}(x, -z).
 \end{aligned} \tag{22}$$

Now we complete the scheme for the case of (symmetrical) absorption at the walls. The reflection factors  $R_i$  in an order of MS are not changed by  $h \rightarrow w$ , except for the sign.

First path:

$$\begin{aligned}
 Q &\xrightarrow[h]{w} R_0 S_0 \begin{cases} \nearrow +R_0 S_2 \rightarrow +R_0 R_4 S_4 \Rightarrow +R_0 R_4 S_6 \rightarrow +R_0 R_4 R_8 S_8 \Rightarrow \dots \\ \searrow -R_0 S_2 \rightarrow -R_0 R_4 S_4 \Rightarrow +R_0 R_4 S_6 \rightarrow +R_0 R_4 R_8 S_8 \Rightarrow \dots \end{cases} \\
 \sum S &= \sum_{i \geq 0} S_i^{(h)} + S_i^{(w)} = 2R_0 S_0 \quad 0 \quad 0 \quad 2R_0 R_4 S_6 \quad 2R_0 R_4 R_8 S_8 \tag{23a} \\
 \Delta S &= \sum_{i \geq 0} S_i^{(h)} - S_i^{(w)} = 0 \quad 2R_0 S_2 \quad 2R_0 R_4 S_4 \quad 0 \quad 0
 \end{aligned}$$

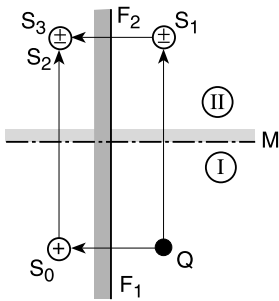
Second path:

$$\begin{aligned}
 Q &\begin{cases} \nearrow +S_1 \rightarrow +R_3 S_3 \Rightarrow +R_3 S_5 \rightarrow +R_3 R_7 S_7 \Rightarrow +R_3 R_7 S_9 \rightarrow \dots \\ \searrow -S_1 \rightarrow -R_3 S_3 \Rightarrow +R_3 S_5 \rightarrow +R_3 R_7 S_7 \Rightarrow -R_3 R_7 S_9 \rightarrow \dots \end{cases} \\
 \sum S &= \sum_{i \geq 0} S_i^{(h)} + S_i^{(w)} = 0 \quad 0 \quad 2R_3 S_5 \quad 2R_3 R_7 S_7 \quad 0 \tag{23b} \\
 \Delta S &= \sum_{i \geq 0} S_i^{(h)} - S_i^{(w)} = 2S_1 \quad 2R_3 S_3 \quad 0 \quad 0 \quad 2R_3 R_7 S_9
 \end{aligned}$$

The most important advantage of the combination MS and PSP is the fact that with it convex corners become tractable; the traditional MS method fails there completely. Since the wedge angle of a couple of walls always is  $\Theta \leq 2\pi$ , the angle between F and M is always  $\leq \pi$ ; the zone (I) in which the scattered field has to be determined is concave; the MS method can be applied there.

In concave corners the application of the PSP possibly produces a higher precision because the MSs have new positions. But this should be checked.

The following sketches mainly assume hard flanks (for simplicity reasons); absorbing flanks will be specially dealt with.



This is the simple case of a source above a plane wall.

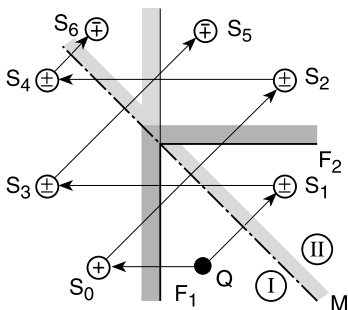
The MSs are shown until interruption by the inside criterion. There is coincidence of  $S_2$ ,  $S_3$  (with the same source factor  $R$  for absorbent  $F_1, F_2$ ).

It is an important question whether such coinciding MS have to be counted a multiple of times or if the MS production is interrupted when coincidence begins.

$S_1, S_2, S_3$  compensate each other in the sum  $\Sigma S$  of  $p_{(I)}$ . The field in (I) is built up by  $Q$  and  $S_0$ , as expected. In the difference  $\Delta S$  of  $p_{(II)}$  the contributions of  $S_1, S_2, S_3$  would sum up if the MSs were used as drawn. As a consequence, the field would be unsteady at  $M$ , which is in contradiction to reality.

Consequently, coincidence of MS with the same source factor  $\Pi R$  must be avoided! Taking this interrupt criterion into account, the field is correctly given by the MS and PSP method. This method thus has a further interrupt criterion, as compared with the traditional MS method. This example also illustrates well the procedure in the MS and PSP method for the evaluation in zone (II): one first evaluates with the significant MSs the scattered field in zone (I) and then mirror-reflects that field at  $M$  into zone (II).

Another instructive example is the concave, rectangular edge.

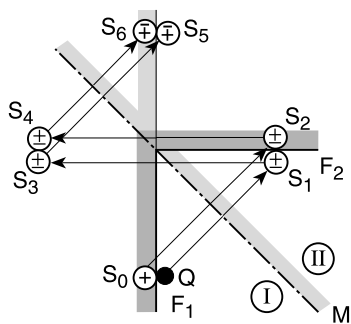


The MSs are drawn as far as is permitted by the inside and coincidence criteria (a further reflection of  $S_5$  at  $F_1$ , which would be permitted by the inside criterion, would produce coincidence with  $S_6$ ).

According to Eq. M.5.(22), the field  $p_I(x, z)$  is created by the superposition of the fields of  $Q, S_0, S_5, S_6$  and the field  $p_{II}(x, -z)$  by the mirror sources  $S_1, S_2, S_3, S_4$ . The boundary

conditions at the flanks  $F_1$ ,  $F_2$  are evidently satisfied. Because both groups of MS can be transformed into each other by a rotation by  $\pi/4$  and a mirror reflection, the field is also steady at  $M$ ; thus it is a solution of the task.

A special case which can easily be understood is obtained if the source  $Q$  approaches the flank  $F_1$ . With a hard flank  $F_1$  again the case of a source above a hard wall  $F_2$  is achieved.

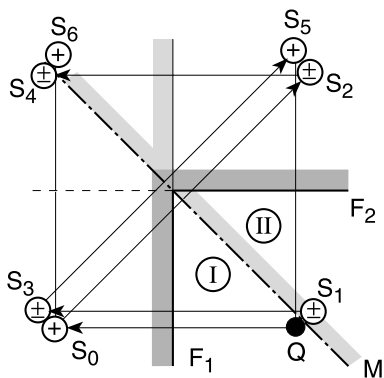


The effective source is a double source  $Q + S_0$ .

As expected, the field is symmetrical relative to  $F_1$  and  $F_2$ . It is also steady at  $M$ .

The field is completely and precisely represented.

In a further limiting case  $Q$  approaches the median plane  $M$ ; the field again is correctly represented, as can be seen from the sketch below.



The MSs are again drawn according to the inside and coincidence criteria.

The source  $Q$  and the MSs marked with  $(+)$  determine the field in zone (I); the MSs marked with  $(\pm)$  contribute (first in zone (I)) to the field in zone (II).

The boundary conditions at  $F_1$ ,  $F_2$  and the condition of steadiness at  $M$  are satisfied.

The examples presented again illustrate the importance of the determination of  $p_{II}$  via the detour over zone (I). The examples contain MSs with  $(\pm)$  in (II). Without the detour, this would mean poles of the field in zone (II). That must be excluded according to the condition of regularity of the scattered field. But with the detour through (I) no problems exist.

### M.5.20 The PSP for Unsymmetrical Absorption

The condition of symmetrical absorption for the application of the PSP to sound fields between couples of walls is a sensible restriction in applications. It will be attempted, therefore, to resolve that restriction, if necessary by an approximation, which, however, should not introduce errors exceeding the errors of the traditional MS method with absorbing walls.

If the flanks are symmetrical, the field in the subtask  $\sigma = h$  is symmetrical with respect to  $M$  (i.e.  $M$  is hard); in the subtask  $\sigma = w$  the field is anti-symmetrical (i.e.  $M$  is soft). Symmetry and anti-symmetry of the fields are solely determined by the source  $Q$  and the auxiliary sources of the PSP. If the walls are different, a new anti-symmetrical part of the field will arise due to the asymmetry of the walls.

It is always possible to compose an unsymmetrical field  $p(x, z)$  from two *geometrically* equal halves (I) and (II) of a wedge with symmetrical and anti-symmetrical field components:

$$\begin{aligned} p(x, z) &= p^{(sy)}(x, z) + p^{(as)}(x, z), \\ p^{(sy)}(x, -z) &= p^{(sy)}(x, z); \quad p^{(as)}(x, -z) = -p^{(as)}(x, z). \end{aligned} \quad (24)$$

From this it follows that:

$$\begin{aligned} p^{(sy)}(x, z) &= \frac{1}{2} (p(x, z) + p(x, -z)), \\ p^{(as)}(x, z) &= \frac{1}{2} (p(x, z) - p(x, -z)). \end{aligned} \quad (25)$$

$M$  by definition is hard for the part  $p^{(sy)}$  and soft for the part  $p^{(as)}$ . Therefore these parts have a common characteristic with  $p_s^{(h)}$ ,  $p_s^{(w)}$  of the PSP with symmetrical flanks.

Further, the field  $p(x, z)$  shall satisfy the boundary conditions at the flanks  $F_1, F_2$ :

$$\begin{aligned} p(F_1) &= p^{(sy)}(F_1) + p^{(as)}(F_1) \stackrel{!}{=} v_{\perp}(F_1)/G_1, \\ p(F_2) &= p^{(sy)}(F_1) - p^{(as)}(F_1) \stackrel{!}{=} v_{\perp}(F_2)/G_2. \end{aligned} \quad (26)$$

In these boundary conditions the parts  $p^{(sy)}$ ,  $p^{(as)}$  appear in the same combination as  $p_s^{(h)}$ ,  $p_s^{(w)}$  in the PSP. Thus, from formal considerations one arrives at an approximation for the PSP when applied to wall couples with different absorption of the flanks.



Complete the PSP for acoustically different walls as follows:

- Apply in the PSP for the evaluation of the field  $p_{(I)}$  in zone (I) the sum

$$p_{(I)}(x, z) = Q + \frac{1}{2} \left( \sum_i p_{s,i}^{(h)}(x, z) + \sum_i p_{s,i}^{(w)}(x, z) \right)$$

using for the reflection factors the admittance of the flank  $F_1$ .

- Apply in PSP for the evaluation of the field  $p_{(II)}$  in zone (II) the difference

$$p_{(II)}(x, z) = \frac{1}{2} \left( \sum_i p_{s,i}^{(h)}(x, -z) - \sum_i p_{s,i}^{(w)}(x, -z) \right)$$

using for the reflection factors the admittance of the flank  $F_2$ .

This rule creates a field which

- satisfies the wave equation in the approximation of the MS method for absorbent walls,
- satisfies the source condition,
- satisfies the boundary conditions at  $F_1, F_2$ ,
- but is not steady at M for unsymmetrical absorption.

It is possible to derive a better approximation which is steady also at M, but it is more complicated to handle and therefore will not be presented here. The errors of the above approximation are of the same order as the errors of the conventional MS method.

### M.5.21 A Global Application of the PSP

Most auditoriums have a constructional plane of symmetry M, so the room as a whole satisfies the condition for the application of the PSP with symmetrical couples of walls, also with respect to absorption.

That means: one solves the task of field evaluation twice in the half of the room containing source Q; once when M is assumed to be hard and once when M is assumed to be soft.

The computational advantage can be easily quantified in 2D (similar relations hold in 3D). The room is supposed to have  $n_w$  walls. In the subtasks of the PSP will appear the following numbers of walls (M included):

- $n_w/2 + 2$  walls, if M ends on both sides on walls;
- $(n_w - 1)/2 + 2$  walls, if M ends on one side with a wall, and on the other side in a corner;
- $n_w/2$  walls, if M ends on both sides in corners.

With this remark ends that part which is concerned with the evaluation of the stationary sound field in rooms. It should be noted that the methods described yield complex sound pressures in field point P. The computations will be somewhat simplified if one is satisfied with the magnitudes  $|p_q|$  of the contributions of the effective sources (MS and corner sources). This is mostly done in room acoustical papers, although it is impossible to conclude from  $|p_q|$  to  $|p(P)|$  (the magnitude of a sum mostly is different from the sum

of magnitudes...). We shall be confronted with that difference in the next section which deals with the determination of the room reverberation using the results of the field evaluation. Although reverberation is a non-stationary process, it should be possible to evaluate the most important room acoustical qualifier, the reverberation time, from the results of a computational field model. In doing that, one will be confronted with some lack of definition of reverberation in common textbook descriptions.

### M.5.22 Reverberation Time with Results of the MS Method

The method described above delivers the stationary, monochromatic field of a stationary, harmonic source in a room. It returns the complex sound pressure  $p(P)$  at a point  $P$ , i.e. with magnitude and phase.

The most important room acoustical qualifier is the reverberation time; it is described in the literature (more or less) by:

“The reverberation time is the elapsed time for a decay of the sound pressure (or sound pressure level) by 60 dB after termination of a stationary sound excitation.”

It is tacitly understood that “sound pressure” means the *magnitude* of the sound pressure, and in most experimental determinations of the reverberation time *band noise* is used with the sound pressure magnitude of an *average* over the bandwidth. It is not mentioned (but it is important, as we will see below) that the rectification of the received signal (for the magnitude and band average) implies averaging over time intervals.

The reverberation process is non-stationary; our field evaluation is for stationary fields. Therefore one needs a “switch-off model” for the evaluations. It should be recalled in that context that the sound field in the room is created in the MS method (as well as in the modified MS and PSP methods) by equivalent sources, which means that, after the equivalent sources have been installed in the right places and with the right amplitudes, the walls of the room can be taken away. The equivalent sources radiate into the free space!

One can imagine the distributed sources as a network of loudspeakers driven by the same signal generator. The network lines contain attenuators which model the source factors  $\Pi R$ . If the signal generator is switched off, all loudspeakers are switched off instantly, but the sound waves radiated before switch-off still propagate. This model has the advantage that the boundary conditions at the walls are satisfied every time because as long as a sound wave from a source hits a wall, the sound wave from its daughter source with that wall will be present also.

The end of the contribution of a source  $q$  arrives at  $P$  at a time  $t$  after switch-off:

$$t = \frac{\text{dist}(q, P)}{c_0} = \frac{k_0 \cdot \text{dist}(q, P)}{\omega}; \quad \omega = 2\pi/T_p, \quad (27)$$

$$\frac{t}{T_p} = \frac{k_0 \cdot \text{dist}(q, P)}{2\pi}.$$

Here  $T_p$  is the time period of the harmonic sound wave. It is reasonable to measure  $t$  in units of periods  $T_p$ .

Imagine all evaluated MSs (and their field contributions  $p_s(P)$ ) sorted with increasing  $k_0 \cdot \text{dist}(q, P)$  and indexed in this order with a number  $s$  ( $s = 0$  may represent the original source  $Q$ ). After some elapsed time  $t/T_p$ , those contributions that are still travelling from their source to  $P$  will be summed at  $P$ . The decay curve  $L(P)$  at  $P$  expressed as sound pressure level is therefore:

$$L(t/T_p) = 10 \cdot \lg \left| \sum_{k_0 \cdot \text{dist}(q(s), P) \geq 2\pi \cdot t/T_p} p_s(P) \right|^2. \quad (28)$$

With increasing  $t/T_p$  the summation is performed over smaller and smaller remainders of the set of effective MSs. This evaluation will therefore produce a steeper slope of  $L(t/T_p)$  at the end of a time interval of observation when this end approaches fewer and fewer remaining MSs. This increase in slope must not be confused with the slope produced by the decreasing amplitudes of MS with increasing distance (due to geometrical and/or acoustical reduction) but is a consequence of the finite size of the set of MSs.

Equation M.5.(28) is a direct transcription of the reverberation process defined above verbally. Formation of the magnitude and square is applied to the sum of contributions. Instead of proceeding on the  $t/T_p$  axis in unit steps of  $s$ , one can proceed in steps  $\Delta t/T_p$ . Contributions within the interval  $\Delta t/T_p$  are summed up (linearly!). Below we shall see that the decay curves thus evaluated have only a slight similarity to an expected reverberation curve. This is a consequence of an improper definition. A clearer definition describes the reverberation as the “decay of the average energy density”. The (effective) energy density implies the square of the sound pressure; averaging is performed over directions of the sound intensity and time intervals which are short compared with the reverberation time. Because tacitly the contributions of different sources are also assumed to be incoherent, the contributions of sources to the energy density can be added and they are proportional to the magnitude squared of their contributions  $p_q(P)$  to the sound pressure  $p(P)$ :

$$E_q(P) = \frac{1}{2\rho_0 c_0^2} |p_q(P)|^2. \quad (29)$$

This definition leads to a reverberation curve

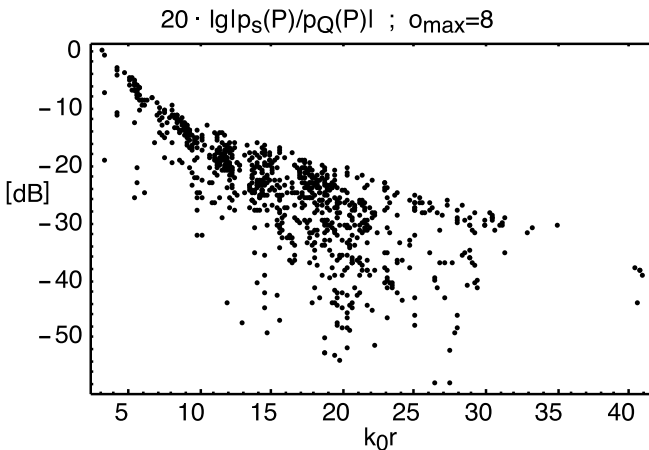
$$L(t/T_p) = 10 \cdot \lg \left[ \frac{1}{2\rho_0 c_0^2} \sum_{n > \frac{t/T_p}{\Delta t/T_p}} \frac{1}{\Delta s} \sum_{k_0 \cdot \text{dist}(q(s), P) \leq 2\pi \cdot \Delta t/T_p} |p(s)|^2 \right]. \quad (30)$$

The outer sum indicates summation in steps of time intervals  $\Delta t/T_p$  in which  $\Delta s$  sources are found and that this outer summation includes a decreasing number  $n$  of such steps. The inner sum forms a squared average (with the factor  $1/\Delta s$ ) of the contributions in a time interval (this summation is skipped if  $\Delta s = 0$ ).

### M.5.23 A Room with Concave Edges as an Example

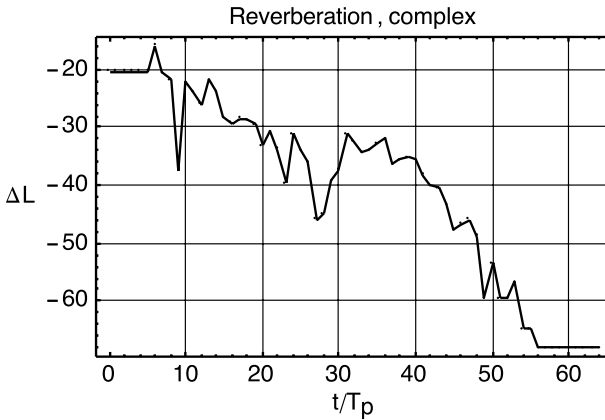
We take the concave room of the previous [Sect. M.5.10](#) as a model room, with the same positions of the source  $Q$  and the receiver  $P$  as there. The evaluation of the mirror sources is performed for orders up to  $o_{\max} = 8$ . The lower limit of  $|IIR|$  was set to  $\text{limit} = 0.01$ ; the upper limit for the distances was with  $d_{\max} = 100 \cdot \text{dist}(Q, P)$  set so high that it did not exclude a legal source. This produces 837 effective sources.

The next diagram shows over  $k_0 r$ , with  $r = \text{dist}(q, P)$ , the sound pressure levels  $p_q(P)$  of the contributions at  $P$ , relative to the contribution  $p_Q(P)$  of the original source  $Q$ . The cloud of points has a typical triangular shape: the upper border has an approximately constant slope after a somewhat steeper slope for smaller  $k_0 r$ . The lower border lines are not so well defined, because there the points are disperse. The upwards trending lower border line towards the right is predominantly determined by the termination with  $o_{\max}$ . One can expect that the upper border line has some similarity with the reverberation curve.

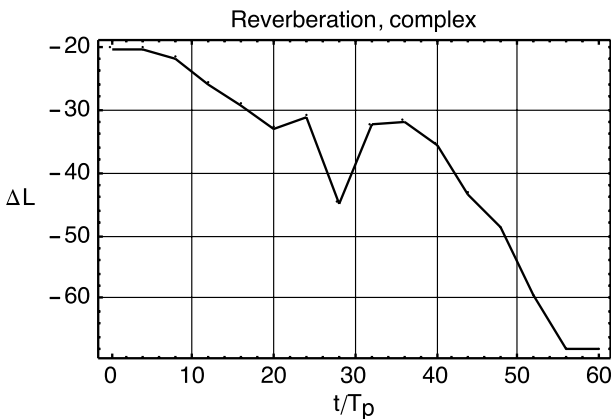


Levels of sound pressure contributions at  $P$  of the original and mirror sources up to order  $o_{\max} = 8$

The evaluation of Eq. M.5.(28) returns the reverberation curves of the next figures which differ from each other only in the value used for the time interval  $\Delta t/T_p$ . They do not resemble reverberation curves with which one is acquainted.



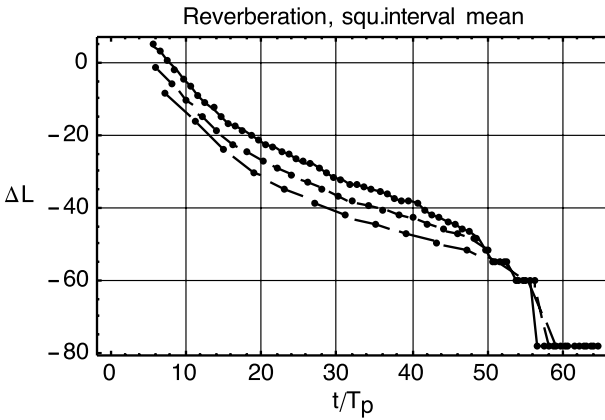
Summation of complex contributions, with time interval  $\Delta t/T_p = 1$



Summation of complex contributions, with time interval  $\Delta t/T_p = 4$

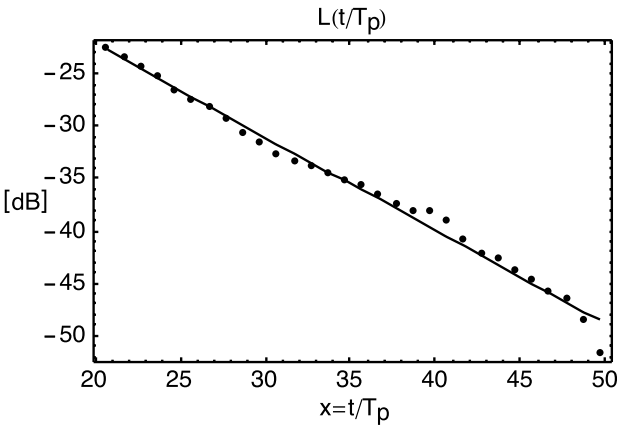
The next diagram combines results of the evaluation of Eq. M.5.(30) with squared averaging in time intervals, again for different time intervals  $\Delta t/T_p$  (within which now an averaging of squared magnitudes takes place); the values of the curves from high to low are  $\Delta t/T_p = 1, 2, 4$ . The points represent centres of the time intervals. The constant factor is omitted.

Except for the steep ends of the curves, which come from the termination of the MS evaluation with  $\alpha_{\max}$ , as explained above, the curves now represent common reverberation curves. They have a steeper “early reverberation” and not so steep “late reverberation”. The choice of  $\Delta t/T_p$  may influence to some degree the value of the reverberation time obtained from such curves, for example as the coefficient of a linear regression through the points within a given interval of observation for  $t/T_p$ .



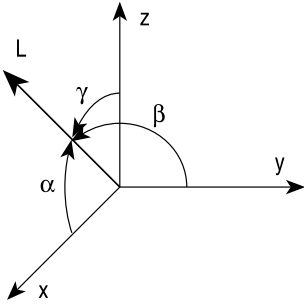
Reverberation curves with Eq. M.5.(30), for different values  $\Delta t/T_p = 1, 2, 4$  (from high to low)

The last diagram combines the points of the reverberation curve for  $\Delta t/T_p = 1$  with the linear regression within the interval  $20 \leq t/T_p \leq 50$ . The reverberation time  $T_r$  in units of  $T_p$  is  $T_r/T_p = 67.46$ .



## Appendix 1: Geometrical Subtasks

A three-dimensional, right-handed Cartesian co-ordinate system  $x, y, z$  is assumed. Points, lines and planes will be considered in 3D. Corresponding relations in 2D are obtained either by setting one co-ordinate to a zero value, identically, or by easy direct derivations. Walls are defined by a list of subsequent edge points  $W = \{E_1, E_2, \dots\}$ ; the sequence of the edges  $E_e$  in the list is such that they define a rotation which with the direction towards the interior of the room forms a right-handed system. Below, mostly not the polygon of a wall is considered, but the plane which contains the wall.



The direction angles  $\alpha$ ,  $\beta$ ,  $\gamma$  of an oriented line  $L$  are the angles between the axes and the line.

(1) Distance  $d$  between two points  $P_1(x_1, y_1, z_1)$ ,  $P_2(x_2, y_2, z_2)$ :

$$d_{PP} = \sqrt{(x_2 - x_1)^2 + (y_2 - y_1)^2 + (z_2 - z_1)^2}. \quad (\text{A.1})$$

(2) Direction cosines of the line from  $P_1(x_1, y_1, z_1)$  to  $P_2(x_2, y_2, z_2)$ :

$$\cos \alpha = \frac{x_2 - x_1}{d_{PP}}; \quad \cos \beta = \frac{y_2 - y_1}{d_{PP}}; \quad \cos \gamma = \frac{z_2 - z_1}{d_{PP}}. \quad (\text{A.2})$$

(3) Cosine of the angle  $\varphi$  between two lines:

The directions of the lines given by their direction angles  $\alpha_i$ ,  $\beta_i$ ,  $\gamma_i$ .

$$\cos \varphi = \cos \alpha_1 \cos \alpha_2 + \cos \beta_1 \cos \beta_2 + \cos \gamma_1 \cos \gamma_2. \quad (\text{A.3})$$

(4) Normal form  $A \cdot x + B \cdot y + C \cdot z + D = 0$  of a plane:

The plane is given by three points  $P_1$ ,  $P_2$ ,  $P_3$  on it. A possible form of the plane equation (coming from a zero value of the vector triple product of the vectors  $(P, P_1)$ ,  $(P_2, P_1)$ ,  $(P_3, P_1)$ ) is:

$$\begin{vmatrix} x - x_1 & y - y_1 & z - z_1 \\ x_2 - x_1 & y_2 - y_1 & z_2 - z_1 \\ x_3 - x_1 & y_3 - y_1 & z_3 - z_1 \end{vmatrix} = 0, \quad (\text{A.4})$$

whence follow the parameters  $A$ ,  $B$ ,  $C$ ,  $D$ :

$$\begin{aligned} A &= y_1(z_2 - z_3) + y_2(z_3 - z_1) + y_3(z_1 - z_2), \\ B &= -x_1(z_2 - z_3) - x_2(z_3 - z_1) - x_3(z_1 - z_2), \\ C &= x_1(y_2 - y_3) + x_2(y_3 - y_1) + x_3(y_1 - y_2), \\ D &= x_1(y_3 z_2 - y_2 z_3) + y_1(x_2 z_3 - x_3 z_2) + z_1(x_3 y_2 - x_2 y_3). \end{aligned} \quad (\text{A.5})$$

(5) Reduced normal form  $a \cdot x + b \cdot y + c \cdot z + d = 0$  of a plane:

$$\begin{aligned} a &= \frac{A}{\sqrt{A^2 + B^2 + C^2}}; & b &= \frac{B}{\sqrt{A^2 + B^2 + C^2}}; \\ c &= \frac{C}{\sqrt{A^2 + B^2 + C^2}}; & d &= \frac{D}{\sqrt{A^2 + B^2 + C^2}}. \end{aligned} \quad (\text{A.6})$$

This reduced normal form should not be confused with Hesse's normal form:

$$a' \cdot x + b' \cdot y + c' \cdot z - p = 0,$$

$$a' = \frac{A}{\pm\sqrt{A^2 + B^2 + C^2}}; \quad b' = \frac{B}{\pm\sqrt{A^2 + B^2 + C^2}}; \quad c' = \frac{C}{\pm\sqrt{A^2 + B^2 + C^2}}; \quad (A.7)$$

$$p = \frac{D}{\pm\sqrt{A^2 + B^2 + C^2}} \geq 0,$$

where the sign of the root is taken so that  $p$  is positive. This additional convention in Hesse's normal form makes it unsuited for inside checks.

The parameters  $a, b, c$  of the reduced normal form are the direction cosines of the normal vector on the plane (pointing to the interior side).

(6) *Foot point*  $P = (x, y, z)$  of a point  $P_1 = (x_1, y_1, z_1)$  on a plane:

The "foot point"  $P$  is the orthogonal projection of  $P_1$  on a plane. Let the plane be given by the parameters of its reduced normal form:

$$\begin{aligned} x &= (b^2 + c^2)x_1 - a(d + by_1 + cz_1), \\ y &= (a^2 + c^2)y_1 - b(d + ax_1 + cz_1), \\ z &= (a^2 + b^2)z_1 - c(d + ax_1 + by_1). \end{aligned} \quad (A.8)$$

(7) *Mirror point*  $P = (x, y, z)$  of a point  $P_1 = (x_1, y_1, z_1)$  on a plane:

$$\text{Let } P_F \text{ be the foot point of } P_1 \text{ on the plane. Then } P = 2 \cdot P_F - P_1. \quad (A.9)$$

(8) *Direction cosines of intersection line of two planes:*

The planes  $W_i$  be given by the parameters  $a_i, b_i, c_i, d_i$  of their reduced normal form:

$$\begin{aligned} \cos \alpha &= \frac{\Delta_1}{\Delta}; \quad \cos \beta = \frac{\Delta_2}{\Delta}; \quad \cos \gamma = \frac{\Delta_3}{\Delta}; \\ \Delta_1 &= \begin{vmatrix} b_1 & c_1 \\ b_2 & c_2 \end{vmatrix}; \quad \Delta_2 = \begin{vmatrix} c_1 & a_1 \\ c_2 & a_2 \end{vmatrix}; \quad \Delta_3 = \begin{vmatrix} a_1 & b_1 \\ a_2 & b_2 \end{vmatrix}; \quad \Delta = \sqrt{\Delta_1^2 + \Delta_2^2 + \Delta_3^2}. \end{aligned} \quad (A.10)$$

The rotation  $W_1 \rightarrow W_2$  and the direction of the intersection line form a right-handed system.

(9) *Point of intersection*  $X = (x, y, z)$  of a line through two points  $P_i = (x_i, y_i, z_i)$  with a plane:

Let the plane  $W$  be given by the parameters  $a, b, c, d$  of its reduced normal form:

$$\begin{aligned} x &= -d(x_1 - x_2) + b(x_2y_1 - x_1y_2) + c(x_2z_1 - x_1z_2)/xx, \\ y &= -d(y_1 - y_2) + a(x_1y_2 - x_2y_1) + c(y_2z_1 - y_1z_2)/xx, \\ z &= -d(z_1 - z_2) + a(x_1z_2 - x_2z_1) + b(y_1z_2 - y_2z_1)/xx, \\ xx &= a(x_1 - x_2) + b(y_1 - y_2) + c(z_1 - z_2). \end{aligned} \quad (A.11)$$



(10) *Foot point*  $P = (x, y, z)$  of a point  $P_1 = (x_1, y_1, z_1)$  on the intersection line of two planes  $W_1, W_2$ :

Let the planes  $W_i$  be given by the parameters  $a_i, b_i, c_i, d_i$  of their reduced normal form:

$$\begin{aligned} x &= (\Delta_3(b_1d_2 - b_2d_1) + \Delta_2(c_2d_1 - c_1d_2) + \Delta_1 \cdot (\Delta_1x_1 + \Delta_2y_1 + \Delta_3z_1)) / \Delta^2, \\ y &= (\Delta_3(a_2d_1 - a_1d_2) + \Delta_1(c_1d_2 - c_2d_1) + \Delta_2 \cdot (\Delta_1x_1 + \Delta_2y_1 + \Delta_3z_1)) / \Delta^2, \\ z &= (\Delta_2(a_1d_2 - a_2d_1) + \Delta_1(b_2d_1 - b_1d_2) + \Delta_3 \cdot (\Delta_1x_1 + \Delta_2y_1 + \Delta_3z_1)) / \Delta^2 \end{aligned} \quad (A.12)$$

with  $\Delta$  and  $\Delta_i$  from Eq. (A.10).

(11) *Bisectrice plane between two intersecting planes*  $W_1, W_2$ :

Let the planes  $W_i$  be given by the parameters  $a_i, b_i, c_i, d_i$  of their reduced normal form. The parameters of the bisectrice plane (containing the intersection line) are:

$$a = (a_1 + \lambda a_2); \quad b = (b_1 + \lambda b_2); \quad c = (c_1 + \lambda c_2); \quad d = (d_1 + \lambda d_2); \quad \lambda = \pm 1. \quad (A.13)$$

(12) *Two planes parallel or anti-parallel:*

Parallel: the three parameters  $a, b, c$  of the reduced normal form are pairwise equal;  
anti-parallel: two of the parameters are pairwise equal, the other differs in sign.

(13) *Distance between two antiparallel planes:*

Let the planes  $W_i$  be given by the parameters  $a_i, b_i, c_i, d_i$  of their reduced normal form.

$$\text{Distance } \delta: \quad \delta = |d_1 - d_2|. \quad (A.14)$$

(14) *Inside check of a point*  $P = (x, y, z)$  relative to a plane given by three points  $P_i = (x_i, y_i, z_i)$ :

The check is performed with and returns:

$$\text{sign} \begin{vmatrix} x - x_1 & y - y_1 & z - z_1 \\ x - x_2 & y - y_2 & z - z_2 \\ x - x_3 & y - y_3 & z - z_3 \end{vmatrix} = \begin{cases} +1 & \text{if } P \text{ is inside } W \\ 0 & \text{if } P \text{ is on } W \\ -1 & \text{if } P \text{ is outside } W, \end{cases} \quad (A.15)$$

where  $|\dots|$  indicates a determinant and  $\text{sign}(x)$  checks the sign of  $x$ .

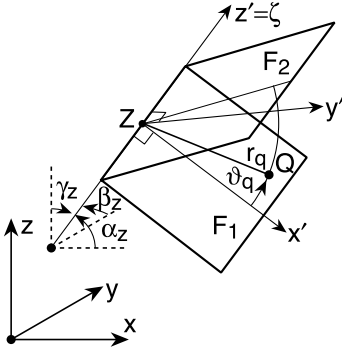
(15) *Inside check of a point*  $P = (x, y, z)$  relative to a plane given by its reduced normal form parameters:

The check is performed with and returns

$$\text{sign}(a \cdot x + b \cdot y + c \cdot z + d) = \begin{cases} +1 & \text{if } P \text{ is inside } W \\ 0 & \text{if } P \text{ is on } W \\ -1 & \text{if } P \text{ is outside } W. \end{cases} \quad (A.16)$$

(16) *Co-ordinate transformation:*

The system  $x, y, z$  is rotated and shifted as shown in the sketch. The new axis  $z' = \zeta$  in the applications is the intersection line of two planes  $F_1, F_2$ ; the new origin  $Z$  is the foot point of the original source  $Q$  on the intersection line.



$x', y', z'$  is a right-handed system, like  $x, y, z$ . The rotation  $F_1 \rightarrow F_2$  forms with  $z'$  a right-handed system.

The transformation  $x, y, z \rightarrow x', y', z'$  is done by:

$$\begin{pmatrix} x' \\ y' \\ z' \end{pmatrix} = \begin{pmatrix} \cos \alpha_x & \cos \beta_x & \cos \gamma_x \\ \cos \alpha_y & \cos \beta_y & \cos \gamma_y \\ \cos \alpha_z & \cos \beta_z & \cos \gamma_z \end{pmatrix} \cdot \begin{pmatrix} x - x_z \\ y - y_z \\ z - z_z \end{pmatrix}. \quad (\text{A.17})$$

The inverse transformation  $x', y', z' \rightarrow x, y, z$  is done (with the transposed matrix) by:

$$\begin{pmatrix} x \\ y \\ z \end{pmatrix} = \begin{pmatrix} \cos \alpha_x & \cos \alpha_y & \cos \alpha_z \\ \cos \beta_x & \cos \beta_y & \cos \beta_z \\ \cos \gamma_x & \cos \gamma_y & \cos \gamma_z \end{pmatrix} \cdot \begin{pmatrix} x' \\ y' \\ z' \end{pmatrix} + \begin{pmatrix} x_z \\ y_z \\ z_z \end{pmatrix}. \quad (\text{A.18})$$

## Appendix 2: Algorithm of Mirror Source Scouting in Concave Rooms

“Scouting” means finding the positions of mirror sources. In “concave rooms” with only concave corners the traditional mirror source (MS) scouting is applied. This method can also be applied in moderately convex rooms in which the wedge angles of convex corners are close to  $\sim \pi$ . Then a wall, possibly shaded by a convex corner, will mostly be excluded from the chain of MS production by the inside criterion. The sound field evaluation with the traditional MS method consists of five main parts:

- input and evaluation of geometrical room data (e.g. wall co-ordinates, wall centres, normal form parameters of wall planes);
- input and evaluation of acoustical wall parameters (e.g. wall admittance values, normal incidence reflection factors);
- scouting for legal mirror sources.  
Selection of effective mirror sources from list of legal mirror sources;
- evaluation of sound field contributions of MSs in field point P.

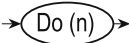
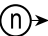
## Symbols:

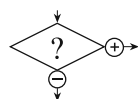
$\text{list} = \{\text{item}_1, \text{item}_2, \dots, \text{item}_n, \dots\}$  list of items with item counter  $n$ ;

$\text{list}[[m]]$  list member number  $m$ ;

$\text{tab}[o]$  a table (or list) with index  $o$ ;

$((n))$  see entry number  $n$  in Appendix 1.

 entry to a loop with loop counter  $n$ , ending at 



branching after test ? for positive or negative test result.

## Room input:

$\{W_w\} = \{W_1, W_2, \dots, W_w, \dots\}$  list of walls  $W_w$ , index  $w$ ; defines the room; the sequence of walls is arbitrary;

$W_w = \{E_1, E_2, \dots, E_e, \dots\}$  list of edges  $E_e$ , index  $e$ ; defines a wall; the sequence of edges forms a right-handed system with wall normal towards interior room side;

$E_e = \{x_e, y_e, z_e\}$  list of Cartesian co-ordinates of edge  $E_e$ .

## Derived room parameters:

$\{C_w\} = \{C_1, C_2, \dots, C_w, \dots\}$  list of wall centres  $C_w$ ;

$\{\dots, \{a_w, b_w, c_w, d_w\}, \dots\}$  coefficients of reduced normal form of walls  $W_w$ ; see Appendix 1, no. ((5)).

## Acoustical wall parameters:

$\{G_w\} = \{G_1, G_2, \dots, G_w, \dots\}$  list of (normalised) wall admittance values;

$\{|R_{0w}|\} = \{\dots, |R_{0w}|, \dots\}$  list of reflexion factor magnitudes of walls  $W_w$ ;  $|R_{0w}| = |1 - G_w|/|1 + G_w|$  for normal sound incidence; may be used for scout interrupt checks.

## Input of source and immission point co-ordinates:

$Q = \{x_Q, y_Q, z_Q\}$  co-ordinates of original source  $Q$ ;

$P = \{x_P, y_P, z_P\}$  co-ordinates of field point  $P$ .

## Input for scouting interrupt:

$\text{omax} =$  upper limit of MS order  $o = 0, 1, \dots, o_{\max}$ ;  $o = 0$  belongs to original source  $Q$ ;

$\text{dmax} =$  upper limit of distance  $\text{dist}(q, P)$  between a MS and  $P$ ;

$\text{limit} =$  lower limit of magnitude of source amplitude factor  $|IIR|$ .

## Goal of scouting:

Output of tables  $\text{tab}[o]$  for MS orders  $o = 0, 1, 2, \dots, o_{hi}$  consisting of MS lists  $q_{list}$  which contain all needed parameters for the evaluation of the mirror sources of the next order  $o + 1$  (if any) and for the evaluation of the field contribution of effective mirror sources in the field point  $P$ :

$q\text{list} = \{q, w, dqP = \text{dist}(q, P), pR = \Pi R(\Theta), \text{flag}\}$

$q$  = co-ordinates of the source (original or mirror);

$w$  = counting index of the “mother wall” if  $q$  is a MS;

$w = 0$  for original source;

$dqP = \text{dist}(q, P)$  = distance from  $q$  to field point  $P$ ;

$pR = \Pi R(\Theta)$  = “source factor” = product of reflection factors  $R(\Theta)$  of increasing orders for sound incidence on  $W_w$  under the angle  $\Theta$  from  $q$ ;

$\text{flag}$  = control flag for source efficiency:

$\text{flag} = 0$ :  $q$  is an efficient source;

$\text{flag} = 1$ :  $q$  is inefficient because  $P$  is not in the field angle  $\angle(q, W_w)$ .

Looping:

The algorithm works with nested loops.

The outer loop runs through the orders  $o = 1, 2, \dots, o_{\max}$  of MS reflection;

the middle loop runs over the sources  $q_s, s = 1, 2, \dots$ , in the table  $\text{tab}[o - 1]$ ;

the innermost loop runs over the wall indices  $w$  of the room list  $\{W_w\}$ .

The source list of the mother source (index  $s$  in  $\text{tab}[o - 1]$ ) is:

$q\text{list}(s) = \{q_s, w_s, dq_sP = \text{dist}(q_s, P), pR_s = \Pi R(\Theta_s), \text{flags}\}$ .

The wanted source list of a daughter source is:

$q\text{list} = \{q, w, dqP = \text{dist}(q, P), pR = \Pi R(\Theta), \text{flag}\}$ .

Break-off criteria for scouting:

- $w = w_s$  back-reflection of daughter source on mother source;
- $q_s$  is not inside  $W_w$ ;
- centre  $C_w$  of mirror wall  $W_w$  is not in field angle  $\angle(q_s, W_{w_s})$ ;
- $|R(\Theta) \cdot \Pi R(\Theta_s)| < \text{limit}$ , i.e. expected field contribution too small by absorption;
- $\text{dist}(q, P) > d_{\max}$ , i.e. field contribution too small by distance;
- $o > o_{\max}$  mirror source order would become too high;
- $\text{tab}[o - 1]$  is empty, i.e. no legal MS of order  $o - 1$  exists.

① Input:

$\{W_w\} = \{W_1, W_2, \dots, W_w, \dots\}$   
 $\{G_w\} = \{G_1, G_2, \dots, G_w, \dots\}$   
 $Q = \{x_Q, y_Q, z_Q\}$   
 $P = \{x_P, y_P, z_P\}$   
 $o_{\max}$   
 $d_{\max}$   
 $\text{limit}$

② Derived input parameters, fixed:

$\text{whi} = \text{number of walls}$   
 $\text{wcenters} = \{C_w\}$   
 $\text{wnormals} = \{\dots, \{a_w, b_w, c_w, d_w\}, \dots\}$   
 $dQP = \text{dist}(Q, P)$   
 $r0list = \{|R_{0w}|\}$

③ Start member  $\text{tab}[0]$  for original source:

$\text{tab}[0] = \{Q, 0, dQP, 1, 0\}$

④ o-loop over orders:  
 $o = 1, \dots, o_{\max}$

Do (o) ← o-loop

⑤ s-loop over sources  $s$  in  $\text{tab}[o-1]$ :

Do (s) ← s-loop

$o=1$

+

$qslist = \text{tab}[0] = \{Q, 0, dQP, 1, 0\}$

−

$qslist = \text{tab}[o-1][[s]] = \{q_s, w_s, \text{dist}(q_s, P), \text{IIR}(\Theta_s), \text{flags}\}$

Room geometry data;  
 admittance of walls;  
 position source  $Q$   
 and field point  $P$ ;  
 limits for order  $o$ ,  
 distances  $\text{dist}(q, P)$ ,  
 MS amplitude in  $P$ .

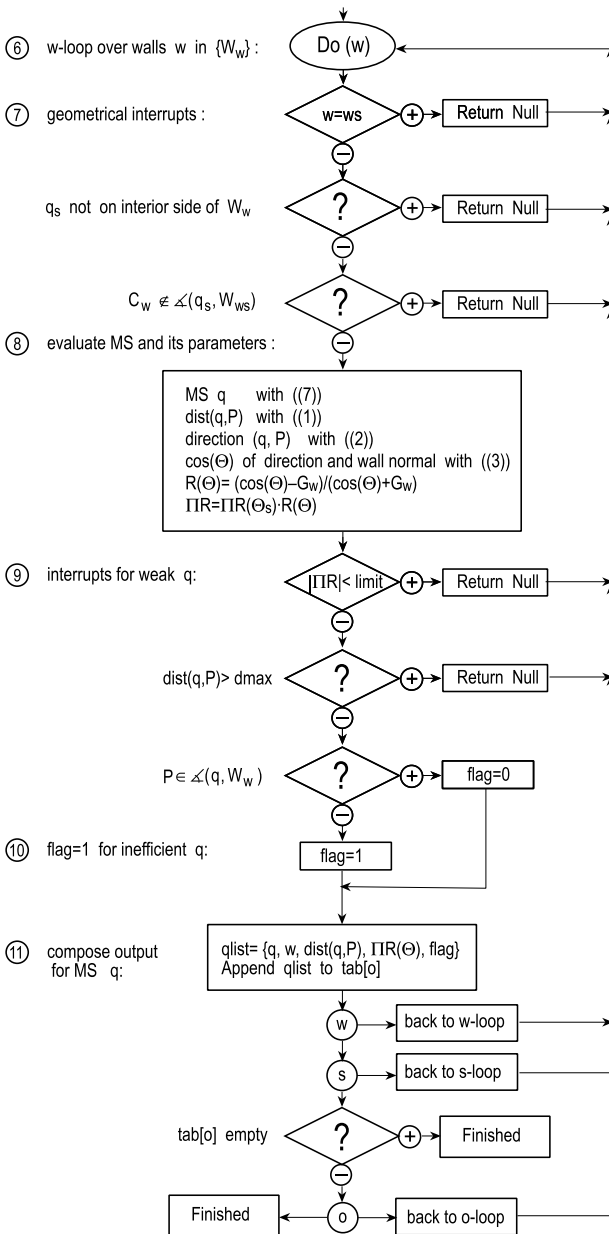
Invariable parameters.

Source list of  
 original source  $Q$ .

Upward looping  
 over order  $o$ .

Looping through  
 sources  $q$  in  $\text{tab}[o-1]$ .

Call source list  
 of source no.  $s$  in  
 $\text{tab}[o-1]$ .



Loop over walls of room.

Jump w-loop if back-reflection.

Jump w-loop if  $q_s$  is not inside wall.

Jump w-loop if centre  $C_w$  of wall  $W_w$  is not in field angle of  $q_s$ .

Evaluate position  $q$ ; distance  $\text{dist}(q, P)$ ; direction cosine of angle of sound incidence from  $q$  on  $W_w$ ; reflection factor  $R(\Theta)$ , amplitude  $IIR$ .

Jump w-loop if  $|IIR|$  is too small.

Jump w-loop if  $q$  is too far from  $P$ .

$q$  is ineffective if  $P$  is not in its field angle; such sources are marked with  $\text{flag} = 1$ .

Compose source list of newly found MS.

Scouting stops if  $\text{tab}[o]$  remains empty.

Scouting is finished.

Evaluation of the sound field in  $P$  by the summed contributions of the MSs in the lists  $\text{tab}[o]$  is easy. The sound field contributions are phased.

## M.6 Ray-Tracing Models

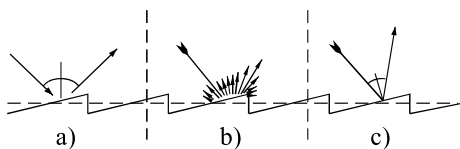
Ray-tracing models are based on geometrical acoustics. Accordingly the wavelengths are considered small compared with characteristic dimensions of the room. Sound is regarded as an energetic process. Calculations of quantities proportional to the sound pressure are estimations with the assumption of:

- broadband stationary or transient signals,
- superposition of energy or other quadratic field quantities.

These assumptions are both related to a consideration of sound energy in terms of a particle rather than a wave. Accordingly, ray tracing cannot be used for simulation of interference effects like standing waves, modes or diffraction.

$\delta$ :	random-incidence scattering coefficient;
$e$ :	ray energy;
$N$ :	number of rays;
$r_d$ :	detector radius;
$\Delta t$ :	sampling interval;
$W$ :	total sound energy in a volume $V$ ;
$z, z_1, z_2$ :	random numbers

Scattering, however, is often accounted for by a statistical approach by means of modelling the statistical case. The statistical case of scattering is described by Lambert's law. The direction of scattered sound is independent of the direction of incidence. Furthermore, the directions of scattering are distributed according to a cosine law, thus resulting in a constant emission of energy into all spatial angles. (In the equivalent phenomenon in optics, a surface with sound scattering according to Lambert's law would be observed with constant light intensity from all directions.) The crucial parameter for surface scattering is the size and the shape of the surface corrugation. Sound wavelengths are distributed from being "large" to "small", compared with the surface corrugations. This fact can be related to assumption of two ideal cases: (a) geometrical reflection and (b) random scattering. Therefore low frequencies are best treated with specular reflections, intermediate frequencies with random scattering and high frequencies with small-scale geometrical reflections.



Reflection from rough surfaces, at low (a), mid (b) and high (c) frequencies

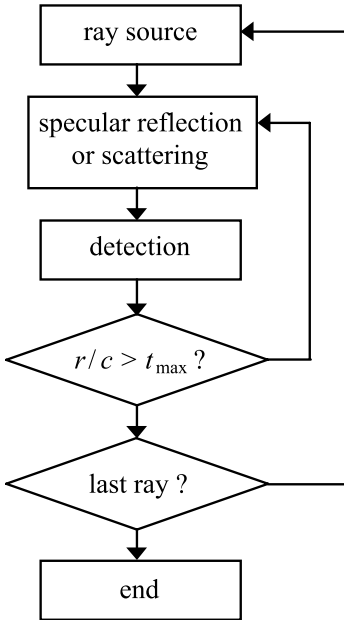
Since reflections in room acoustics and particularly the reverberation process are built up by numerous reflections, the average behaviour is much more important than each individual scattering characteristic. It is thus sufficient to consider a mixed model of

geometrical and diffuse reflections with a “switching” parameter and a random process with appropriate probability distribution. The parameter which decides which model is used is the random-incidence scattering coefficient  $\delta$ :

$$\delta = 1 - \frac{E_{\text{spec}}}{E_{\text{total}}}. \quad (\text{A.18})$$

### Monte Carlo Method:

$N$  rays are radiated from a source point. Typically  $N$  is larger than 10 000. Each ray is carrying a portion of sound energy  $e_0$ . In this method the ray detection is provided by counting the rays hitting a detector (for instance, a sphere with radius  $r_d$ ) and sampling the counts in time intervals  $\Delta t$ .



In a diffuse sound field the expectation value of the energy decay (energy time curve) is:

$$\langle e(t) \rangle = e_0 N (1 - \bar{\alpha})^{\bar{n}t} \frac{\pi r_d^2 c_0 \Delta t}{V} \quad (\text{A.18})$$

with room volume  $V$  and  $\bar{n}$  the mean reflection rate and  $\bar{\alpha}$  the average absorption coefficient of the room (see ➤ Sect. M.4).

Wall absorption can be modelled by energy reduction according to multiplication of the ray energy by  $(1 - \alpha)$ ,  $\alpha$  being the random-incidence absorption coefficient of the wall.

Alternatively, a random number  $z \in [0; 1]$  can be chosen and the ray can be absorbed if  $z < \alpha$ . The probability density that the ray is absorbed at the next wall reflection is:

$$w(\bar{n}t) = (1 - \bar{\alpha})^{\bar{n}t-1} \bar{\alpha}. \quad (\text{A.18})$$



Whether Lambert scattering or specular reflection is used is decided by a random number  $z \in [0; 1]$ . The ray is scattered if  $z < \delta$ .

### *Uncertainty of the Monte Carlo Method*

Relative standard deviation of the statistical counts in the energy decay curve:

$$\frac{\sigma_e}{\langle e \rangle} = \sqrt{\frac{V}{N\pi r_d^2 c_0 \Delta t}} \quad (\text{energy absorption by multiplication}), \text{ or} \quad (\text{A.18})$$

$$\frac{\sigma_e}{\langle e \rangle} = \sqrt{\frac{V}{N(1 - \bar{\alpha})^{\bar{n}t} \pi r_d^2 c_0 \Delta t}} \quad (\text{energy absorption by random absorption}). \quad (\text{A.18})$$

Relative standard deviation of the total energy  $\langle W \rangle$  in the energy decay curve (energy integral):

$$\frac{\sigma_W}{\langle W \rangle} = \frac{\sigma_{|p|^2}}{\langle |p|^2 \rangle} = \sqrt{\frac{A}{8\pi N r_d^2}} \quad (\text{energy absorption by multiplication}), \quad (\text{A.18})$$

which is related to a sound level variation of

$$\sigma_L = 4.34 \sqrt{\frac{A}{8\pi N r_d^2}} \quad (\text{A.18})$$

and

$$\frac{\sigma_W}{\langle W \rangle} = \frac{\sigma_{|p|^2}}{\langle |p|^2 \rangle} = \sqrt{\frac{A}{4\pi N r_d^2}} \quad (\text{energy absorption by random absorption}), \quad (\text{A.18})$$

which is related to a sound level variation of

$$\sigma_L = 4.34 \sqrt{\frac{A}{4\pi N r_d^2}}. \quad (\text{A.18})$$

### **The Cone, Beam or Pyramid Approach:**

In contrast to the Monte Carlo approach of ray tracing, deterministic models of ray tracing are known. Here, the energy time curves are not calculated by counting rays but by determination of ray paths and corresponding geometrical energy reductions. There are several ways of finding physically correct paths by associating the rays with cones or beams with constant solid angle and, thus, increasing spatial spread. In a diffuse sound field the expectation value of each ray energy is calculated by:

$$\langle e(t) \rangle = e_0 \frac{(1 - \bar{\alpha})^{\bar{n}t}}{r^2} \quad (\text{A.18})$$

with  $r$  denoting the distance between the ray source and the receiving point.

Another important difference with the Monte Carlo approach is that the ray energy can be recorded in an arbitrarily high time resolution. In the case of a time resolution

that is sufficient for audio processing, impulse responses can be composed from a set of reflections (or image sources). Each contribution contains a frequency function  $H_j$  which is based on the Fourier transform of the reflection pulse (a Dirac pulse) and multiplied by various frequency functions corresponding to the filter effects on the ray path:

$$H_j = \frac{e^{-jk_0 r_j}}{r_j} H_S H_R H_a \prod_{i=1}^{n_j} R_i \quad (\text{A.18})$$

with  $r_j$  denoting the distance between image source and receiver,  $H_S$  the (directional) spectrum of the source,  $H_R$  the directional head-related transfer function (HRTF, right or left ear) of the receiver person (in the case of binaural processing),  $H_a$  the spectrum of air attenuation, and  $R_i$  the reflection factors of the walls involved in the ray path (or the mirror source). The total binaural impulse response ( $r, l = \text{right, left ear}$ ) is then obtained by inverse Fourier transformation:

$$p_{r,l}(t) = F^{-1} \left\{ \sum_{j=1}^N H_{j,r,l} \right\}. \quad (\text{A.18})$$

### Ray Sources (Deterministic, Random):

Consider an omnidirectional source, with angles of ray direction in relation to source-related spherical co-ordinates  $\varphi, \vartheta$ . The angles are:

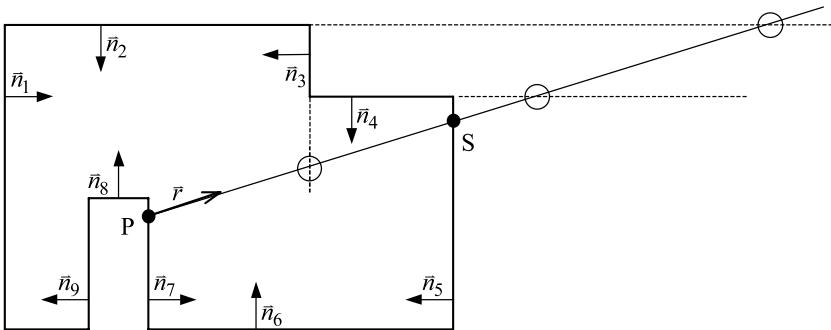
$$\varphi = 2\pi z_1, \quad (\text{A.18})$$

$$\vartheta = \arccos z_2 \quad (\text{A.18})$$

with  $z_1$  the random number of the interval  $[0; 1]$  and  $z_2$  the random number of the interval  $[0; 1]$  independent of  $z_1$ .

Algorithm of reflections (scouting of reflection points):

Last point of ray history  $P$  (vector  $\vec{p}$ ), calculation of next wall hit at point  $S$  (vector  $\vec{s}$ ):



$\vec{n}_i$ : normal vector of wall  $i$  (all wall normal vectors direction towards the interior of the room),  $\vec{r}$ : vector of actual flight direction.

Step 1: Ray must hit the wall plane facing the room (inside)

$$\vec{n}_i \cdot \vec{r} < 0. \quad (\text{A.18})$$

Step 2: All walls passing step 1, ray must hit the next wall in positive flight direction: Calculation of

$$(\vec{p} - \vec{s}) \cdot \vec{r} < 0. \quad (\text{A.18})$$

Step 3: After sorting of distances  $\vec{P}\vec{S}_i$  ( $i = 3, 5, 4, 2$  in the figure above), starting with the nearest wall intersection point, test of “intersection point within polygon” (see ► Sect. M.5). In the case of failure (wall 3 in the figure above), the next point  $S_i$  is to be checked. If a special wall type is defined, “non-shadowing wall”, this test can be skipped for each wall that is non-shadowing. Shadowing walls can block the free line of sight between two arbitrary observer points in the room; non-shadowing walls never block any two arbitrary lines within the room (in the figure above,  $i = 3, 4, 7, 8, 9$  are shadowing walls,  $i = 1, 2, 5, 6$  are non-shadowing walls). It is worthwhile to divide the wall polygons into the two categories.

Step 4: If a non-shadowing wall is reached or if  $S_i$  lies within the wall polygon, the ray is reflected (or absorbed) at wall  $i$ .

Wall scattering (Lambert’s law). Independent of the angle of incidence, the reflection angle  $\Omega(\varphi, \vartheta)$  is randomly chosen according to:

$$w(\vartheta) d\Omega = \frac{1}{\pi} \cos \vartheta d\Omega \quad (\text{A.18})$$

with  $w(\vartheta)$  the probability density of the reflection polar angle  $\vartheta$ . The azimuth angles are equally distributed in  $[0, 2\pi]$ . This is obtained by two independent random numbers  $z_{1,2} \in [0; 1]$  in:

$$\vartheta = \arccos \sqrt{z_1}; \quad \varphi = 2\pi z_2. \quad (\text{A.18})$$

## M.7 Room Impulse Responses, Decay Curves and Reverberation Times

The results of mirror source or ray-tracing algorithms are discrete energy density impulse responses:

$$w(t)\Delta t \approx w(t) dt \propto p^2(t) dt. \quad (\text{A.18})$$

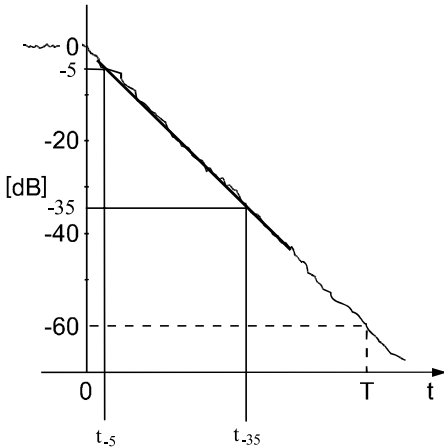
$r^2(t)$ : decay curve;  
 $T_{30}, T_x$ : reverberation time;  
 EDT: Early Decay Time

Decay curve (expectation value for interrupted noise decay):

$$r^2(t) = \int_0^\infty p^2(\tau) d\tau - \int_0^t p^2(\tau) d\tau = \int_t^\infty p^2(\tau) d\tau = \int_\infty^t p^2(\tau) d(-\tau). \quad (\text{A.18})$$

### Reverberation Time $T_{30}$ :

Linear regression from  $-5$  dB to  $-35$  dB of  $10 \log[r^2(t)]$  for determination of  $t_{-5}$  and  $t_{-35}$ , extrapolated to  $-60$  dB by  $T_{30} = 2(t_{-35} - t_{-5})$ .



### General Reverberation Time $T_x$ :

Linear regression from  $-5$  dB to  $-(x + 5)$  dB of  $10 \log[r^2(t)]$  for determination of  $t_{-5}$  and  $t_{-(x+5)}$ , extrapolated to  $-60$  dB by  $T_x = 60/x(t_{-(5+x)} - t_{-5})$ .

### Early Decay Time EDT

(characterising the subjectively perceived reverberance of a room):

Linear regression from  $0.1$  dB to  $-10.1$  dB of  $10 \log[r^2(t)]$  for determination of  $t_{-0.1}$  and  $t_{-10.1}$ , extrapolated to  $-60$  dB by  $EDT = 6(t_{-10.1} - t_{-0.1})$ .

## M.8 Other Room Acoustical Parameters

Impulse responses can be evaluated for calculation of quantities with specific correlation to subjective impressions. All quantities are based on integrals of the squared impulse responses.

- $p(t)$ : sound pressure impulse response;
  - $p_{10}(t)$ : sound pressure impulse response in a reference source-to-receiver distance of 10 m;
  - $p_r(t)$ : sound pressure impulse response obtained for the right ear of a test subject or a dummy head (see Eq. M.6.(A.18));
  - $p_l(t)$ : sound pressure impulse response obtained for a test subject or a dummy head (see Eq. M.6.(A.18));
  - $p_L(t)$ : lateral sound pressure impulse response (figure-of-eight directionality) with its directional null pointed towards the source
- See ➤ Sect. M.4 for definitions of other symbols.

The *sound strength*  $G$  is the relative level between the sound field in the room and the level in a free sound field at 10 m distance, with the power output of the source and the direction of the axis of source and receiver remaining the same:

$$G = 10 \log \left( \int_0^{\infty} |p(t)|^2 dt \Big/ \int_0^{\infty} |p_{10}(t)|^2 dt \right). \quad (\text{A.18})$$

*Definition D* or *early-to-late energy ratio* (characterising the speech intelligibility):

$$D = \int_0^{50 \text{ ms}} |p(t)|^2 dt \Big/ \int_0^{\infty} |p(t)|^2 dt. \quad (\text{A.18})$$

*Clarity*  $C_x$ , early-to-late energy ratio for music ( $x = 80 \text{ ms}$ ) and for speech ( $x = 50 \text{ ms}$ ) (characterising the subjective transparency or speech intelligibility, respectively):

$$C_{80} = 10 \log \int_0^{80 \text{ ms}} |p(t)|^2 dt \Big/ \int_{80 \text{ ms}}^{\infty} |p(t)|^2 dt \text{ [dB]}, \quad (\text{A.18})$$

$$C_{50} = 10 \log \int_0^{50 \text{ ms}} |p(t)|^2 dt \Big/ \int_{50 \text{ ms}}^{\infty} |p(t)|^2 dt \text{ [dB]}. \quad (\text{A.18})$$

Relation between  $D$  and  $C_{50}$ :

$$C_{50} = 10 \log \left( \frac{D}{1 - D} \right). \quad (\text{A.18})$$

*Centre time* (first moment of the impulse response, characterising the reverberance and speech intelligibility):

$$TS = \int_0^{\infty} t |p(t)|^2 dt \Big/ \int_0^{\infty} |p(t)|^2 dt. \quad (\text{A.18})$$

*Lateral energy fraction*: Early lateral sound ratio (characterising the subjective spatial impression “apparent source width”):

$$LF = \int_{5 \text{ ms}}^{80 \text{ ms}} |p_L(t)|^2 dt \Big/ \int_0^{80 \text{ ms}} |p(t)|^2 dt \quad (\text{A.18})$$

with  $p_L(t)$  denoting the sound pressure weighted with a figure-eight directionality, with its directional null pointed towards the source.

*Interaural Cross-Correlation Function*:

$$\text{IACF}_{t_1, t_2}(\tau) = \int_{t_1}^{t_2} p_l(t) \cdot p_r(t + \tau) dt \Big/ \sqrt{\int_{t_1}^{t_2} p_l^2(t) dt \int_{t_1}^{t_2} p_r^2(t) dt}. \quad (\text{A.18})$$

*Interaural Cross-Correlation Coefficient* (characterising the subjective spatial impression):

$$\text{IACC} = \max [\text{IACF}_{-1 \text{ ms}, 1 \text{ ms}}(\tau)]. \quad (\text{A.18})$$

*Late Lateral Sound Level*: (characterising the subjective spatial impression “listener envelopment”) [Bradley/Soulodre (1995)]:

$$\text{LG}_{80}^{\infty} = \int_{80 \text{ ms}}^{\infty} |p_L(t)|^2 dt \Big/ \int_0^{\infty} |p_{10}(t)|^2 dt. \quad (\text{A.18})$$

Estimates of the room acoustical parameters using just the reverberation time can be achieved by consideration of a purely exponential decay [Barron/Lee (1988)]:

Energy integral from time  $t$  to infinity:

$$i_t = (31200T/V) \cdot e^{-13.82t/T} \quad (\text{A.18})$$

with  $r$  denoting the source-to-receiver distance in m,  $T$  the reverberation time in s, and  $V$  the room volume in  $\text{m}^3$ . Contribution of direct, early and late (limit 80 ms) sound energy at a source-to-receiver distance  $r$ :

$$e_d = 100/d^2, \quad (\text{A.18})$$

$$e_e = (31200T/V) \cdot e^{-0.04d/T}(1 - e^{-1.11/T}), \quad (\text{A.18})$$

$$e_l = (31200T/V) \cdot e^{-0.04d/T} \cdot e^{-1.11/T}, \quad (\text{A.18})$$

and accordingly:

$$G = 10 \cdot \log(e_d + e_e + e_l) = 10 \cdot \log(100/d^2 + 31200T/V) \quad (\text{A.18})$$

and

$$C_{80} = 10 \cdot \log[(e_d + e_e)/e_l]. \quad (\text{A.18})$$

In another formulation of the sound strength  $G$  and in agreement with Eq. M.8.(15) and M.8.(16) we find:

$$G = 10 \log \left( \frac{1}{r^2} + 310 \frac{T}{V} \right) + 4.34A/S + 20 = 10 \log \left( \frac{1}{r^2} + \frac{50}{A} \right) + 4.34A/S + 20, \quad (\text{A.18})$$

or, in approximation for large distances  $r$ ,

$$G = 37 - 10 \log A + 4.34A/S; \quad r \gg \sqrt{A}/7 \quad (\text{A.18})$$

with  $A$  the total absorption area and  $S$  the room interior surface area.

Furthermore, the early and late energy densities  $e_e, e_l$  can be calculated as follows, similar to Barron's revised theory [Barron/Lee (1988)], with the  $\bar{n}$  the average reflection rate (see Eq. M.4.(2)) and  $\bar{\alpha}$  the average absorption coefficient (see Eq. M.4.(14)):

$$e_e = \frac{1}{V} \int_{1/\bar{n}}^{(1/\bar{n})+0.05} e^{-13.8t/T} dt + \frac{1}{4\pi c_0 r^2} = \frac{T}{13.8V} \left( e^{-A/S} - e^{-\left(\frac{276}{T} + A/S\right)} \right) + \frac{1}{4\pi c_0 r^2}, \quad (\text{A.18})$$

$$e_1 = \frac{1}{V} \int_{0.05+1/\bar{n}}^{\infty} e^{-13.8t/T} dt = \frac{T}{13.8V} e^{-\left(\frac{276}{T} + A/S\right)}. \quad (\text{A.18})$$

Accordingly, definition D and clarity  $C_{80}$  result in:

$$D = \frac{\frac{T}{13.8V} \left( e^{-A/S} - e^{-\left(\frac{276}{T} + A/S\right)} \right) + \frac{1}{4\pi c_0 r^2}}{\frac{T}{13.8V} e^{-A/S} + \frac{1}{4\pi c_0 r^2}} \approx \frac{\frac{T}{13.8V} \left( 1 - e^{-\frac{276}{T}} \right) + \frac{1}{4\pi c_0 r^2}}{\frac{T}{13.8V} + \frac{1}{4\pi c_0 r^2}}, \quad (\text{A.18})$$

$$C_{80} = 10 \log \frac{\frac{T}{13.8V} \left( e^{-A/S} - e^{-\left(\frac{13.8}{T} 0.08 + A/S\right)} \right) + \frac{1}{4\pi c_0 r^2}}{\frac{T}{13.8V} e^{-\left(\frac{13.8}{T} 0.08 + A/S\right)}} \quad (\text{A.18})$$

$$\approx 10 \log \left( e^{13.8T/V} \left( 1 + \frac{13.8V}{4\pi c_0 r^2 T} \right) - 1 \right) \quad \text{for } A \ll S \quad \text{or} \quad \bar{\alpha} \ll 1,$$

the latter with the influence of the direct field neglected.

## References

- Barron, M., Lee, L.-J.: Energy relations in concert auditoriums. *J. Acoust. Soc. Am.* **84**, 618 (1988)
- Bradley, J. Soulodre, G.A.: Objective measures of listener envelopment. *J. Acoust. Soc. Am.* **98**, 2590 (1995)
- Cremer, L.: Die wissenschaftlichen Grundlagen der Raumakustik, Band I: Geometrische Raumakustik. Hirzel, Stuttgart (1948)
- Kosten, C.W.: The mean free path in room acoustics. *Acustica* **10**, 245 (1960)
- Kuttruff, H.: Room Acoustics, 4th edn. E&FN SPON, London (2000)
- Mechel, F.P.: Schallabsorber, Vol. II, Ch. 10: Sound in capillaries. Hirzel, Stuttgart (1995)
- Mechel, F.P.: Improved mirror source method in room acoustics. *J. Sound Vibr.* **256**, 873–940 (2002)
- Pujolle: Nouvelle Théorie der la Réverberation des Salles. *Rev. Techn. Radio Télévis.* **25**, 254–259 (1972)
- Pujolle: Nouveau point de vue sur l'acoustique des salles. *Revue d'Acoustique* **18**, 21–25 (1972)
- Pujolle: Détermination des dimensions optimales d'une salle. *Revue d'Acoustique* **28**, 13–18 (1974)